Open Access Article

The Detection and Attribution of Northern Hemisphere Land Surface Warming (1850–2018) in Terms of Human and Natural Factors: Challenges of Inadequate Data

by Willie Soon [1,2], Ronan Connolly [1,3,*], Michael Connolly [1,3], Syun-Ichi Akasofu [4], Sallie Baliunas [5,†], Johan Berglund [6], Antonio Bianchini [7,8], William M. Briggs [9], C. J. Butler [10,†], Rodolfo Gustavo Cionco [11,12], Marcel Crok [13], Ana G. Elias [14], Valery M. Fedorov [15], François Gervais [16], Hermann Harde [17], Gregory W. Henry [18], Douglas V. Hoyt [19], Ole Humlum [20], David R. Legates [21,22,†], Anthony R. Lupo [23], Shigenori Maruyama [24,†], Patrick Moore [25], Maxim Ogurtsov [26,27], Coilín ÓhAiseadha [28], Marcos J. Oliveira [29], Seok-Soon Park [30], Shican Qiu [31], Gerré Quinn [32], Nicola Scafetta [33], Jan-Erik Solheim [34,†], Jim Steele [35,†], László Szarka [2], Hiroshi L. Tanaka [36,†], Mitchell K. Taylor [37], Fritz Vahrenholt [38], Víctor M. Velasco Herrera [39] and Weijia Zhang [40] — Hide full author list

結論の要約

地球温暖化のより広範な検出と帰属の問題には、次のような重要な課題が残されていることが明らかになった。
(1)世界の陸地の気温データには、都市化バイアスが依然として大きな問題である。
(2)文献にある多くのTSI時系列のうち、どれが（もしあるとすれば）過去のTSIの正確な推定値なのかがまだ不明である。
(3)1850年以降の温暖化が、ほとんど人為的なものなのか、ほとんど自然なものなのか、あるいは何らかの組み合わせなのか、科学界はまだ確信を持って確定できる状況にない。
これらの科学的課題をどのように解決するかについての提案がなされている。

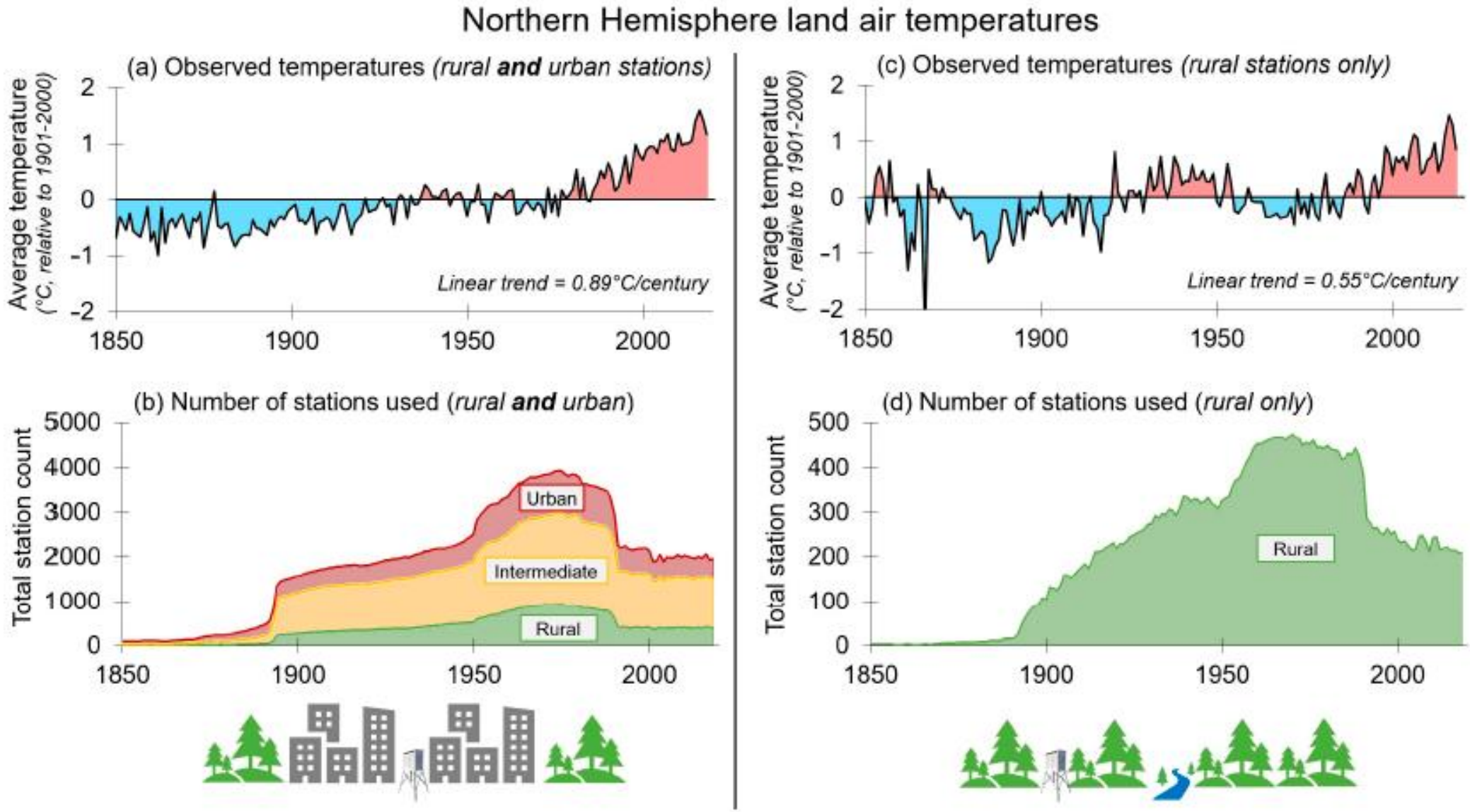
Northern Hemisphere land air temperatures
(a) Observed temperatures (rural and urban stations)
Average temperature (°C, relative to 1901-2000)
Linear trend = 0.89°C/century
(c) Observed temperatures (rural stations only)
Linear trend = 0.55°C/century
(b) Number of stations used (rural and urban)
Total station count
Urban
Intermediate
Rural
(d) Number of stations used (rural only)
1850
1900
1950
2000

Figure 1. Visual comparison of the two different estimates of Northern Hemisphere land air temperature trends (1850–2018) considered in this article. Both series were generated using version 3 of NOAA NCEI's Global Historical Climatology Network (GHCN) dataset. (**a**) The "rural and urban" series is the gridded mean average of all Northern Hemisphere stations regardless of urbanization status. NOAA's homogenized versions of the station records were used. (**b**) The number of stations used for each year of the "rural and urban" series with the relative composition of urban/intermediate/rural for each year indicated via different colors. (**c**) The "rural-only" series uses only rural stations taken from the four regions identified by Connolly et al. (2021) [5]. The homogenization steps described by Connolly et al. (2021) were applied to the station records [5]. (**d**) The number of stations used for each year of the "rural-only" series. Note that the vertical scales are different for (**b**,**d**) since the rural-only series is limited to rural data and therefore only uses 10–15% of the total stations available.

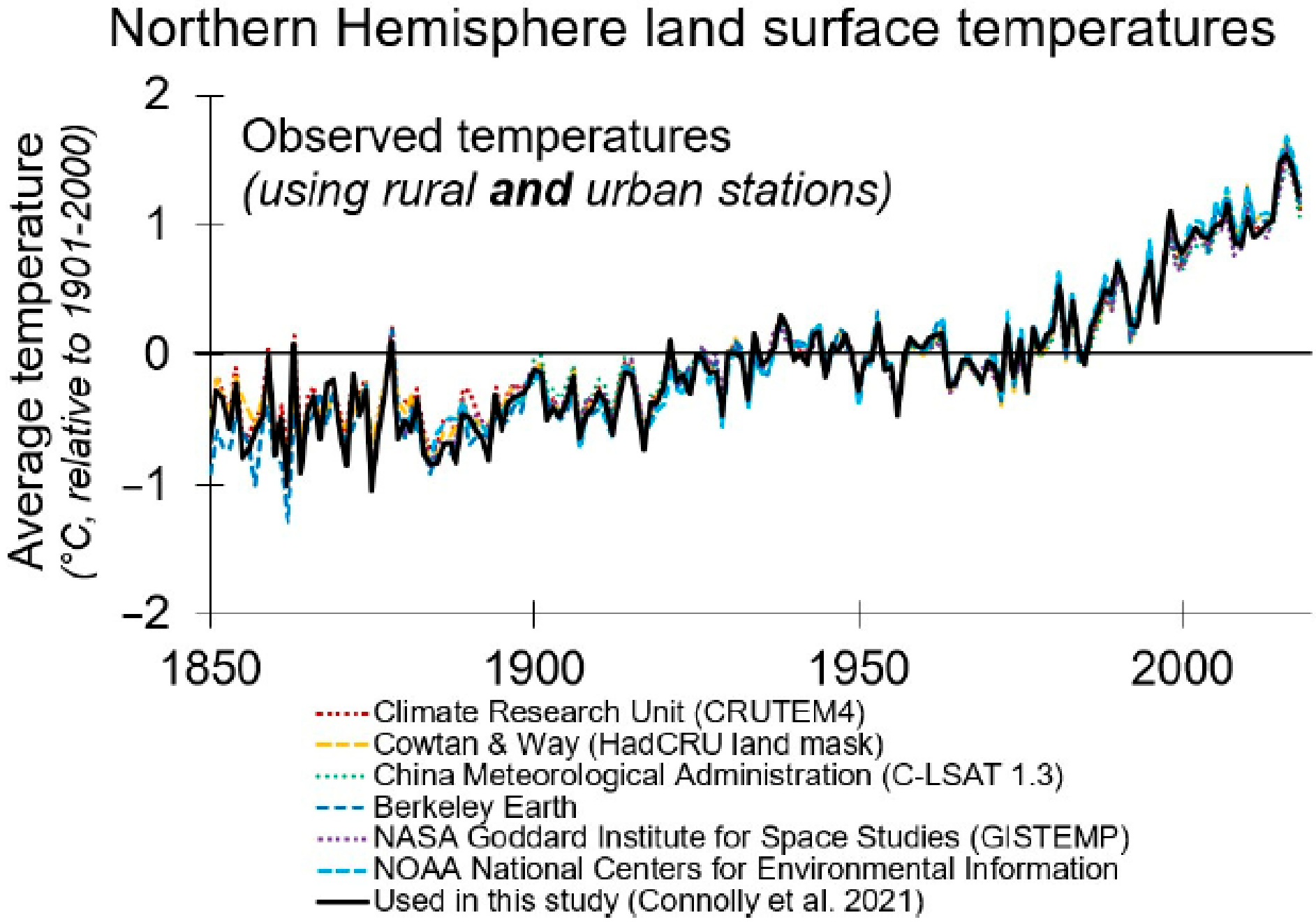
Northern Hemisphere land surface temperatures
Observed temperatures
(using rural and urban stations)
Average temperature
(°C, relative to 1901-2000)
2
1
0
−1
−2
1850
1900
1950
2000
Climate Research Unit (CRUTEM4)
Cowtan & Way (HadCRU land mask)
China Meteorological Administration (C-LSAT 1.3)
Berkeley Earth
NASA Goddard Institute for Space Studies (GISTEMP)
NOAA National Centers for Environmental Information
Used in this study (Connolly et al. 2021)

Figure 2. Visual comparison of the "rural and urban" Northern Hemisphere land surface air temperature time series (1850–2018) used in the article (thick black line) to six other widely used estimates of Northern Hemisphere land surface air temperatures. For more details on these series, see Connolly et al. (2021) [5].

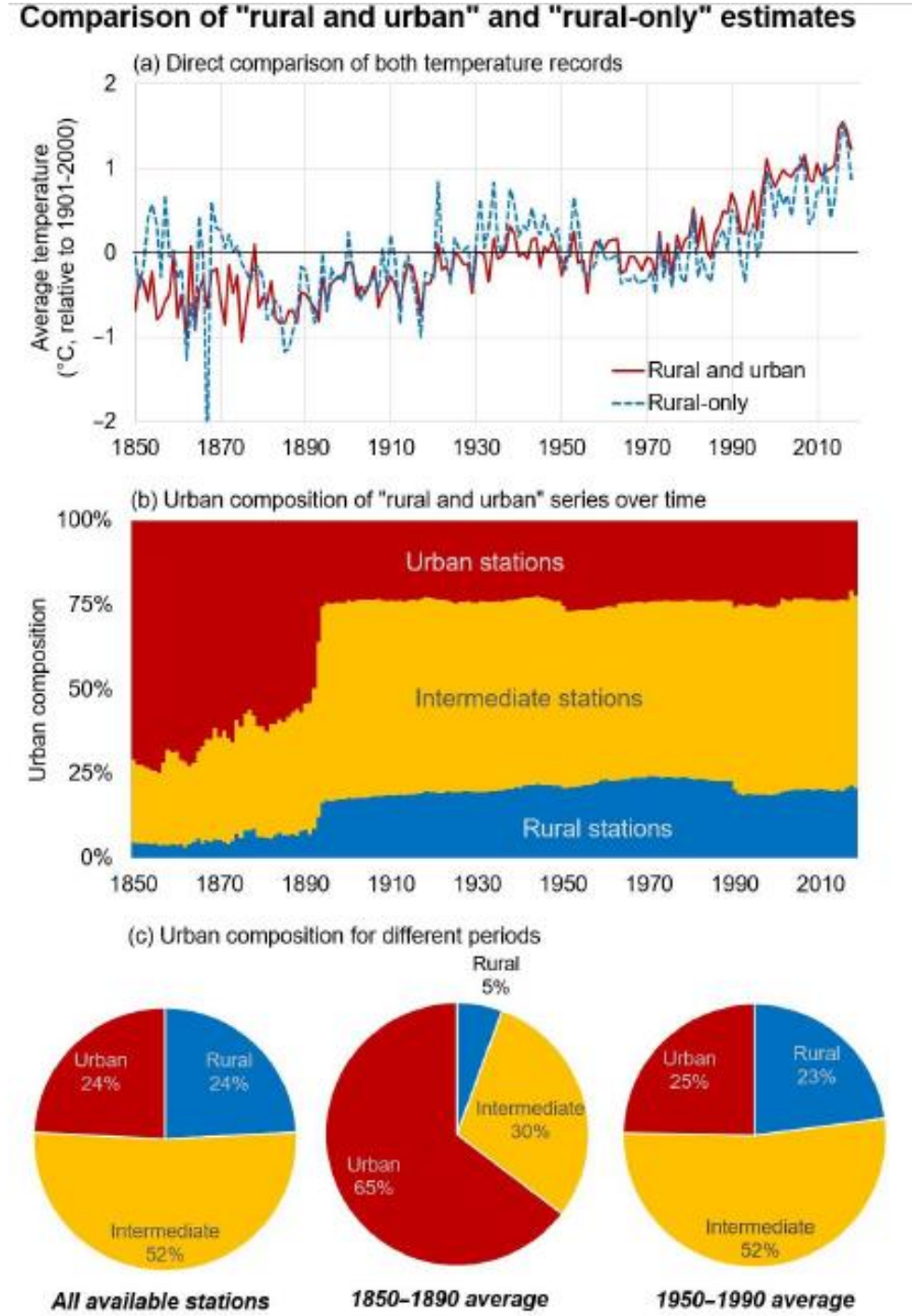
Comparison of "rural and urban" and "rural-only" estimates
(a) Direct comparison of both temperature records
Average temperature (°C, relative to 1901-2000)
2
1
0
−1
−2
1850
1870
1890
1910
1930
1950
1970
1990
2010
Rural and urban
Rural-only
(b) Urban composition of "rural and urban" series over time
Urban composition
100%
75%
50%
25%
0%
Urban stations
Intermediate stations
Rural stations
(c) Urban composition for different periods
Urban 24%
Rural 24%
Intermediate 52%
All available stations
Rural 5%
Intermediate 30%
Urban 65%
1850–1890 average
Urban 25%
Rural 23%
Intermediate 52%
1950–1990 average

Figure 3. Comparison in terms of urban composition of the two Northern Hemisphere land surface air temperature estimates considered in this analysis. (**a**) Both time series of Figure 1 in the same panel for direct comparison. (**b**) The breakdown of urban, intermediate, and rural stations used for each year of the "rural and urban" series. (**c**) Urban composition of the "rural and urban" series averaged over three different time periods: left—all available stations; middle—average breakdown for the 1850–1890 period; right—average breakdown for the 1950–1990 period.

Comparison of "rural and urban" and "rural-only" estimates

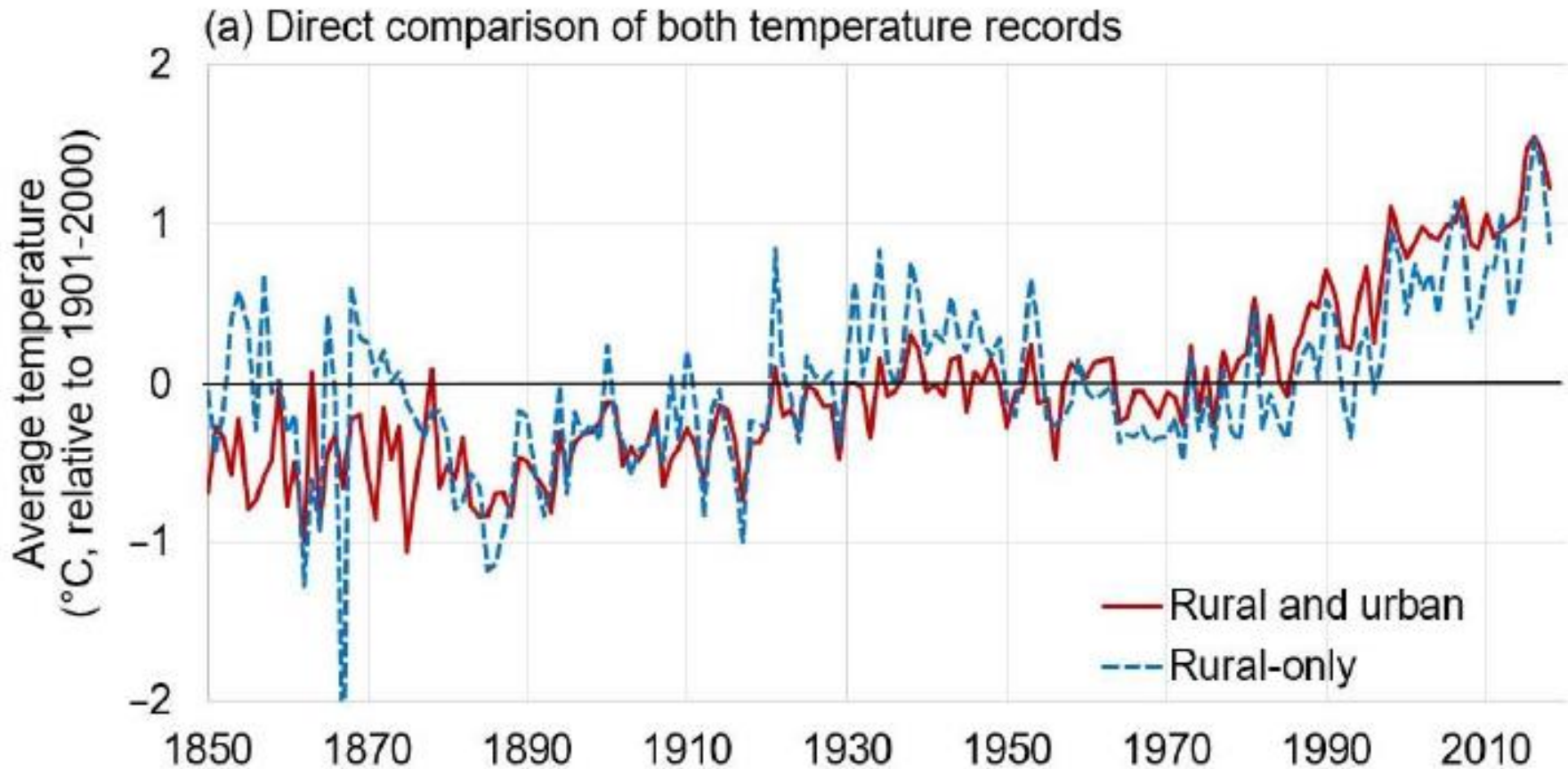

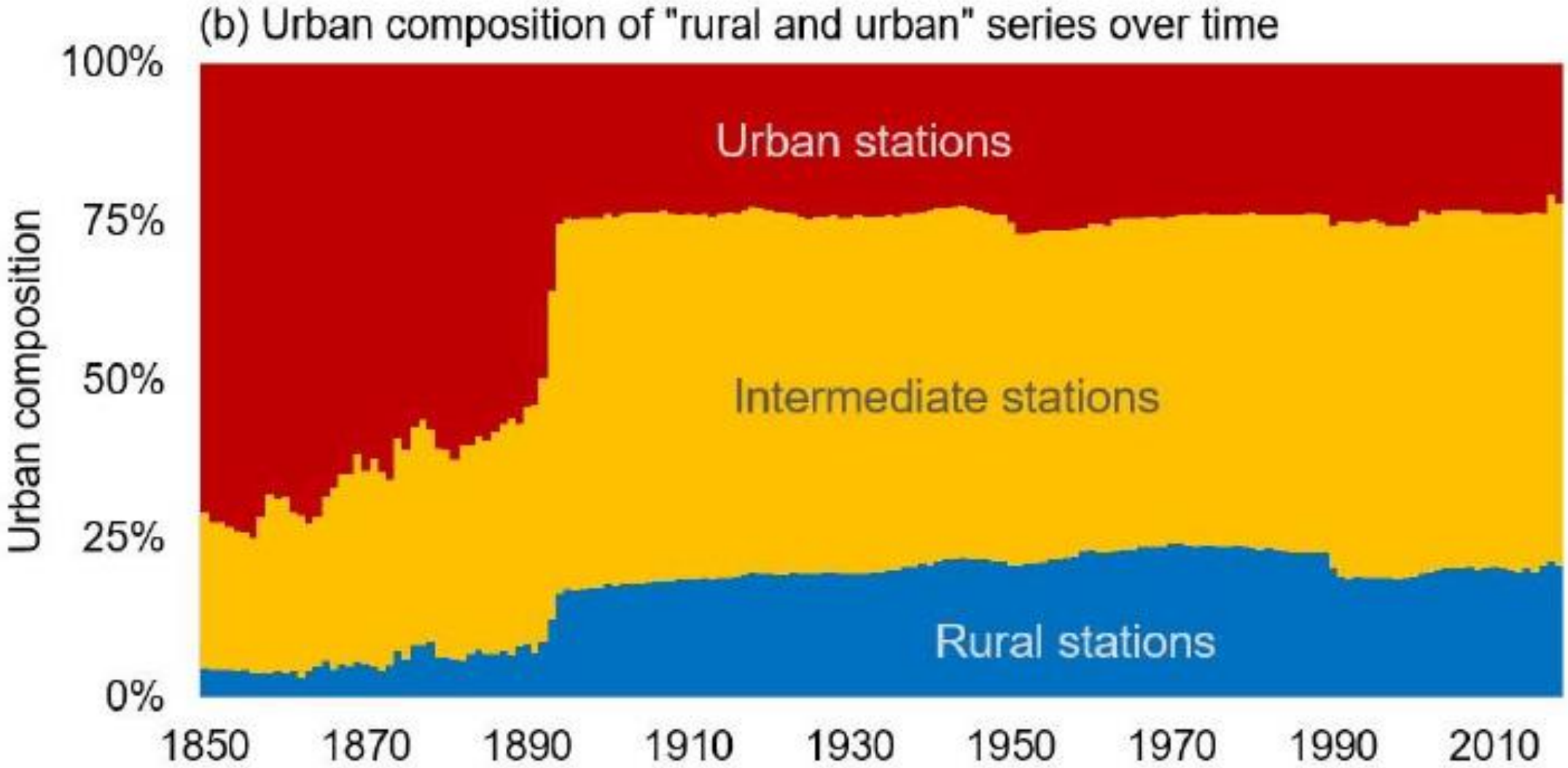
(b) Urban composition of "rural and urban" series over time
Urban composition
100%
75%
50%
25%
0%
Urban stations
Intermediate stations
Rural stations
1850
1870
1890
1910
1930
1950
1970
1990
2010

(c) Urban composition for different periods

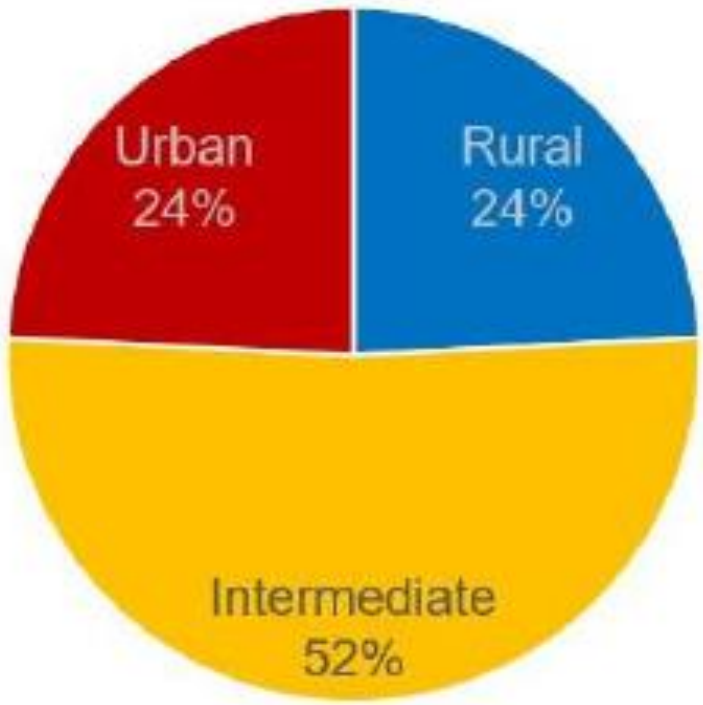

All available stations

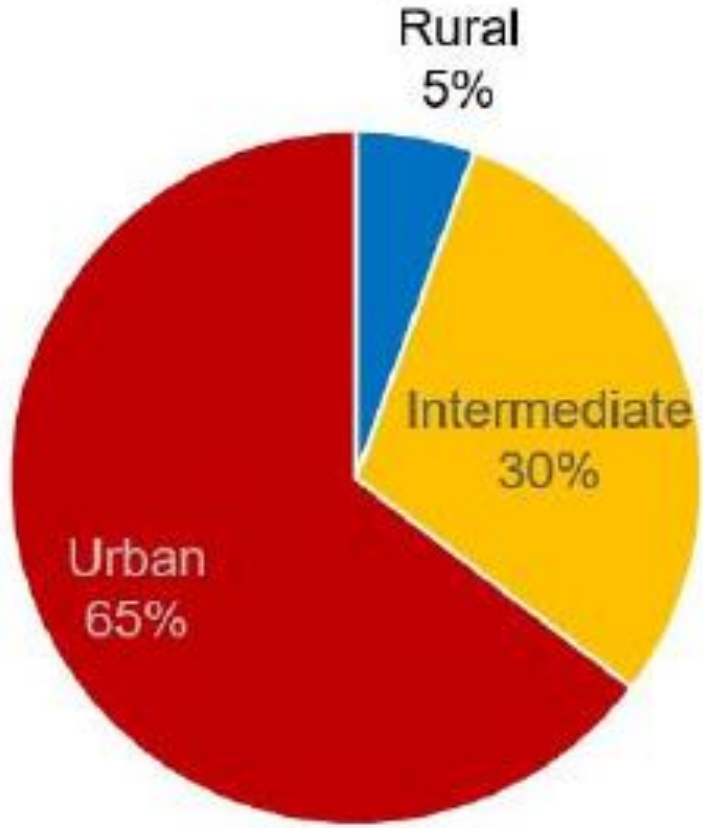

1850–1890 average

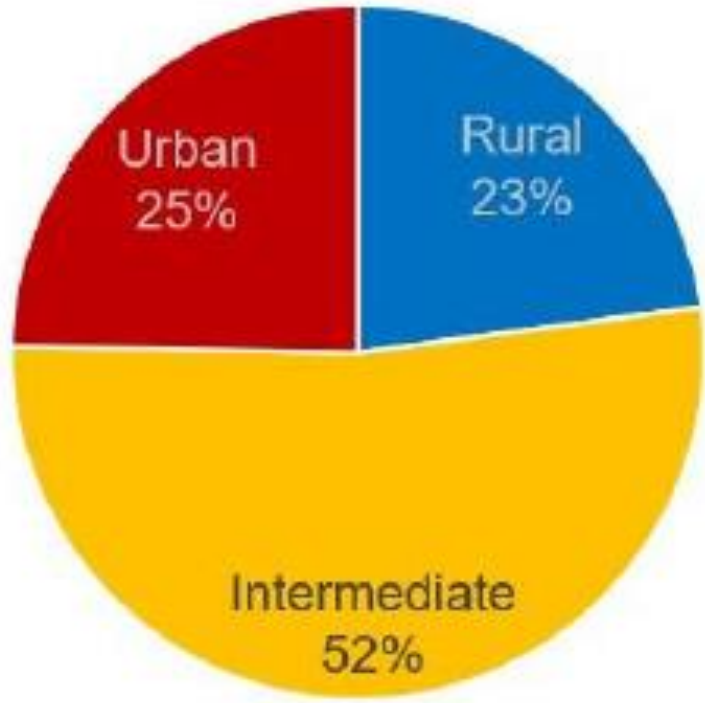

1950–1990 average

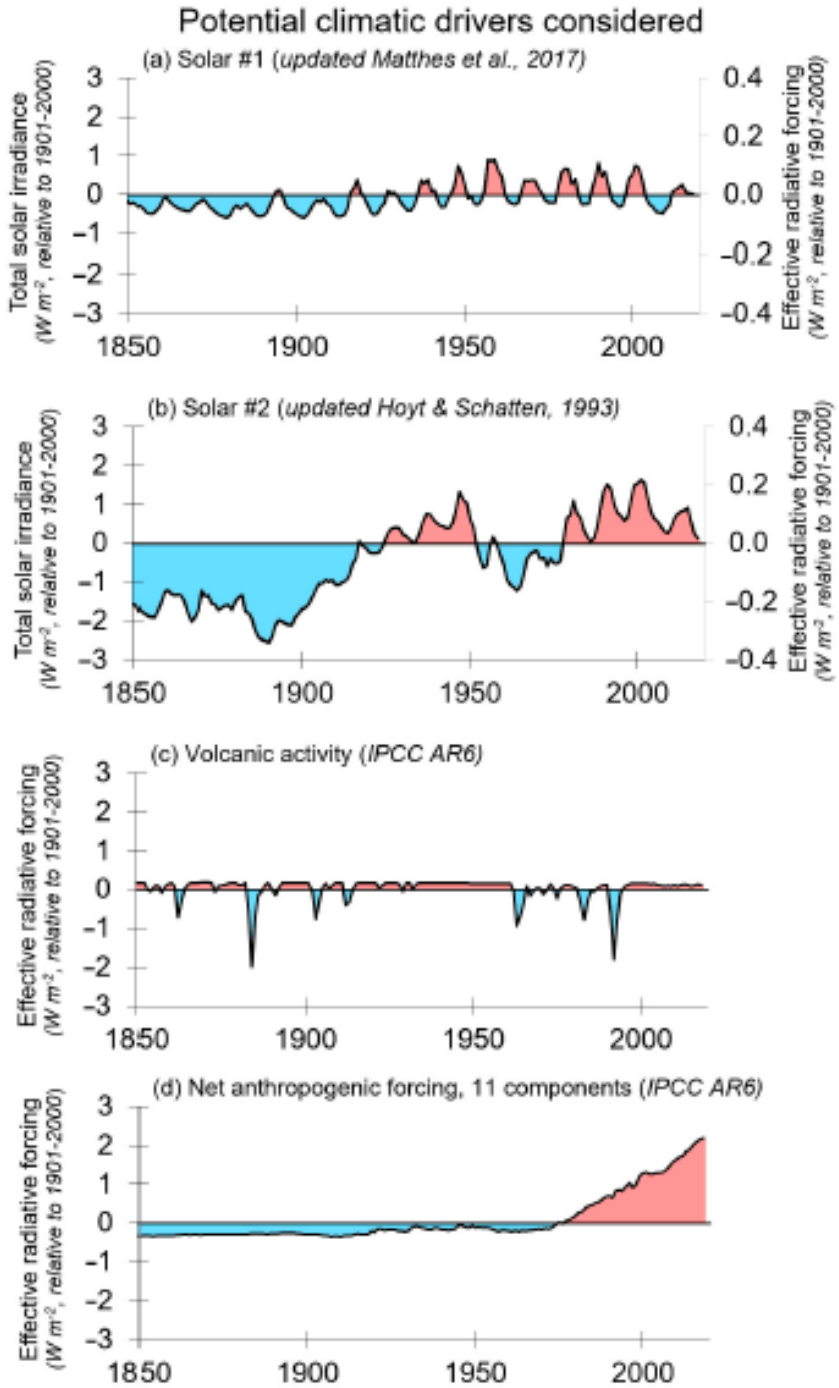
Potential climatic drivers considered
(a) Solar #1 (updated Matthes et al., 2017)
Total solar irradiance (W m-2, relative to 1901-2000)
Effective radiative forcing (W m-2, relative to 1901-2000)
(b) Solar #2 (updated Hoyt & Schatten, 1993)
(c) Volcanic activity (IPCC AR6)
Effective radiative forcing (W m-2, relative to 1901-2000)
(d) Net anthropogenic forcing, 11 components (IPCC AR6)
1850
1900
1950
2000

Figure 4. Time series of the four forcings considered in this analysis. (**a**,**b**) represent two different estimates of solar variability since the mid-19th century; (**c**) plots the volcanic forcing; (**d**) plots the combined anthropogenic forcings. For more details on the two solar activity series, see Connolly et al. (2021) [5]. The volcanic activity and anthropogenic forcing time series are taken from the IPCC AR6 WG1 Annex III dataset [103].

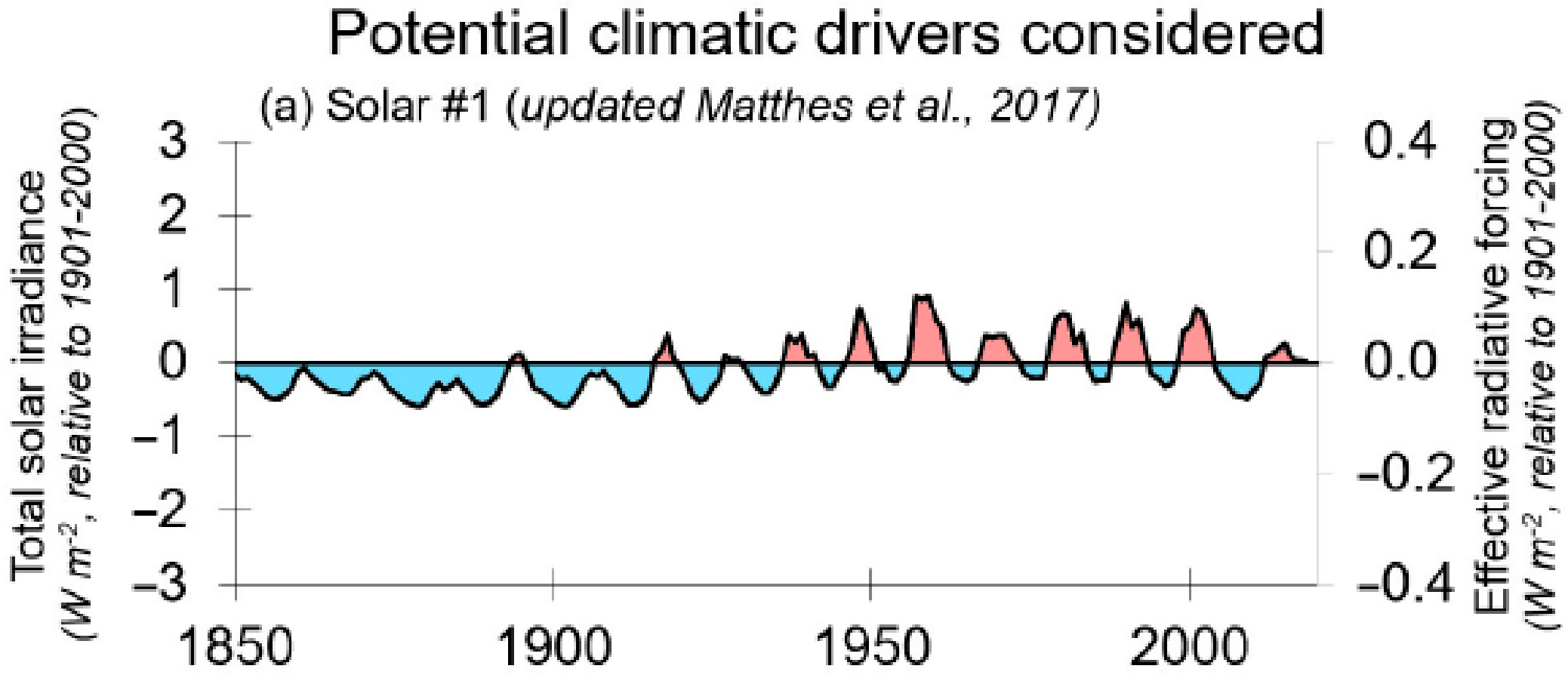
Potential climatic drivers considered
(a) Solar #1 (updated Matthes et al., 2017)
Total solar irradiance
(W m-2, relative to 1901-2000)
3
2
1
0
−1
−2
−3
0.4
0.2
0.0
−0.2
−0.4
Effective radiative forcing
(W m-2, relative to 1901-2000)
1850
1900
1950
2000

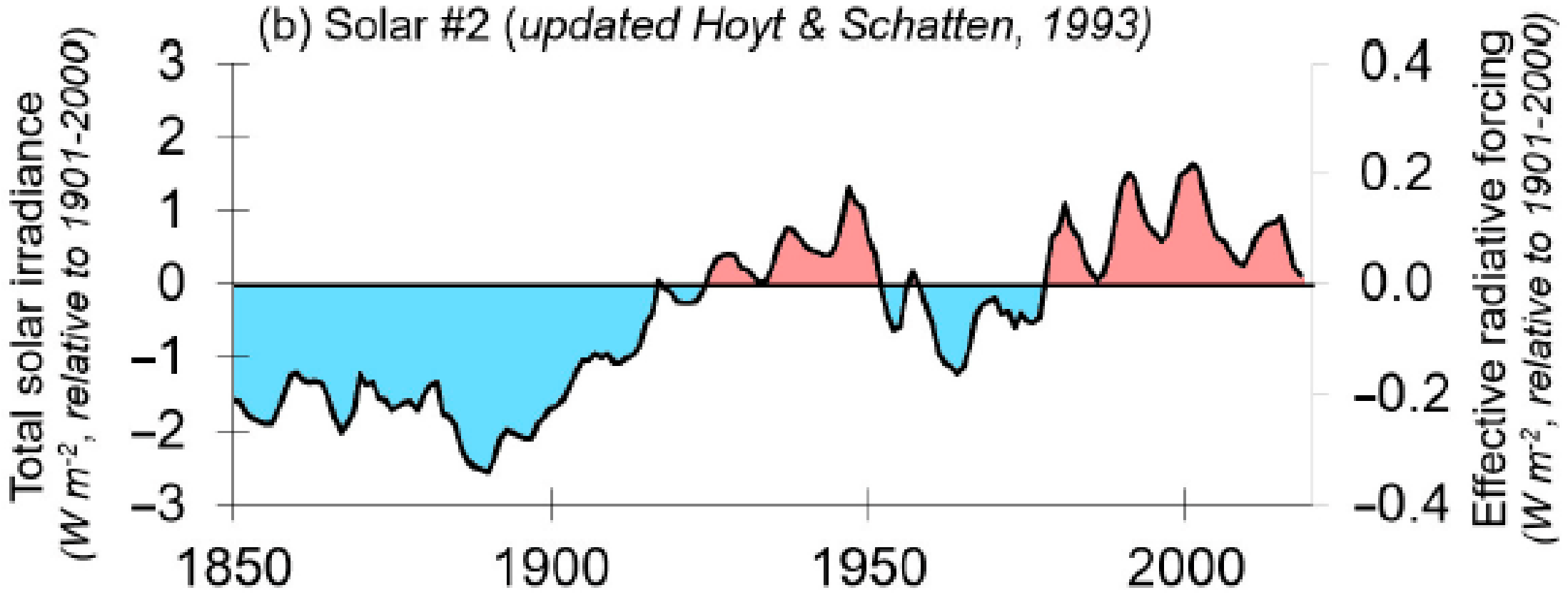
(b) Solar #2 (updated Hoyt & Schatten, 1993)
Total solar irradiance
(W m-2, relative to 1901-2000)
3
2
1
0
−1
−2
−3
Effective radiative forcing
(W m-2, relative to 1901-2000)
0.4
0.2
0.0
−0.2
−0.4
1850
1900
1950
2000

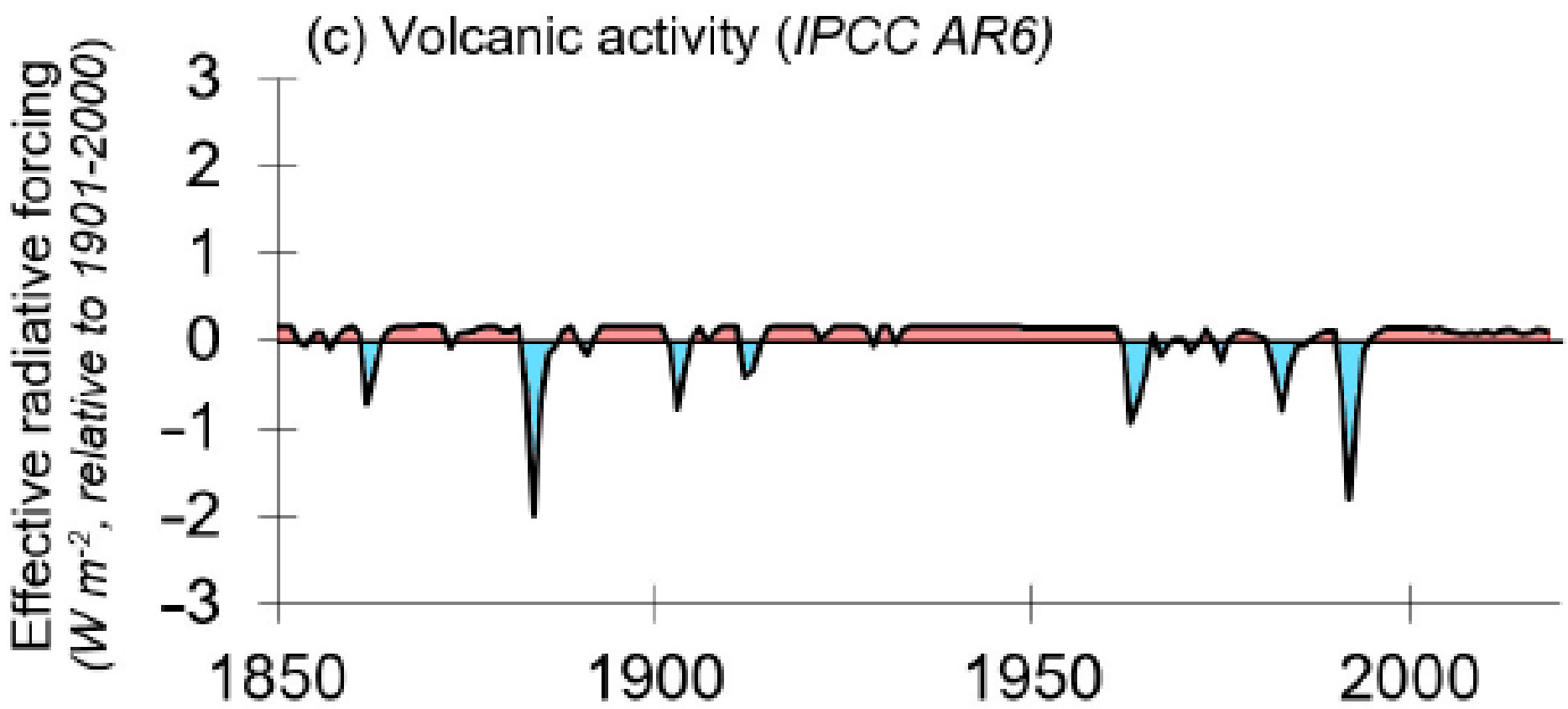
(c) Volcanic activity (IPCC AR6)
Effective radiative forcing
(W m-2, relative to 1901-2000)
3
2
1
0
−1
−2
−3
1850
1900
1950
2000

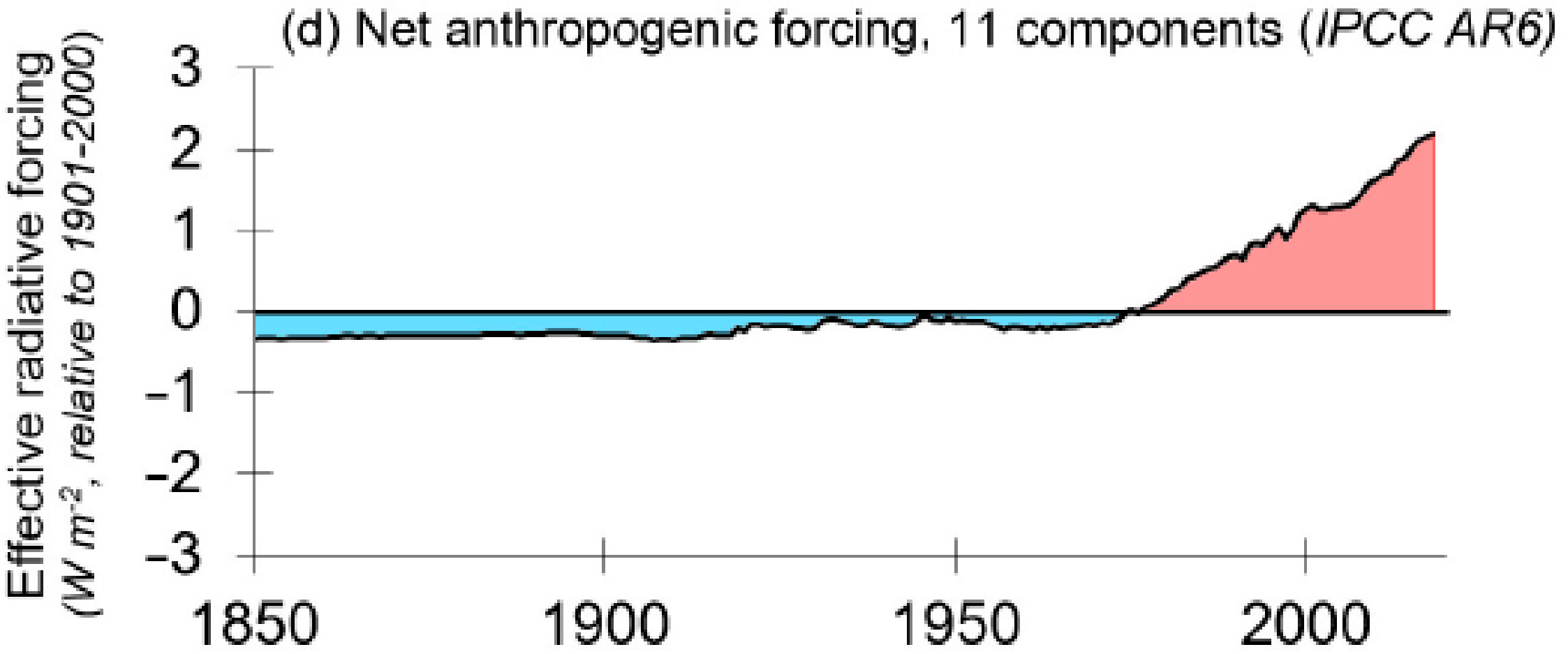
(d) Net anthropogenic forcing, 11 components (IPCC AR6)
Effective radiative forcing
(W m-2, relative to 1901-2000)
3
2
1
0
−1
−2
−3
1850
1900
1950
2000

Fitting results for each component *Using 1850–2018 data*

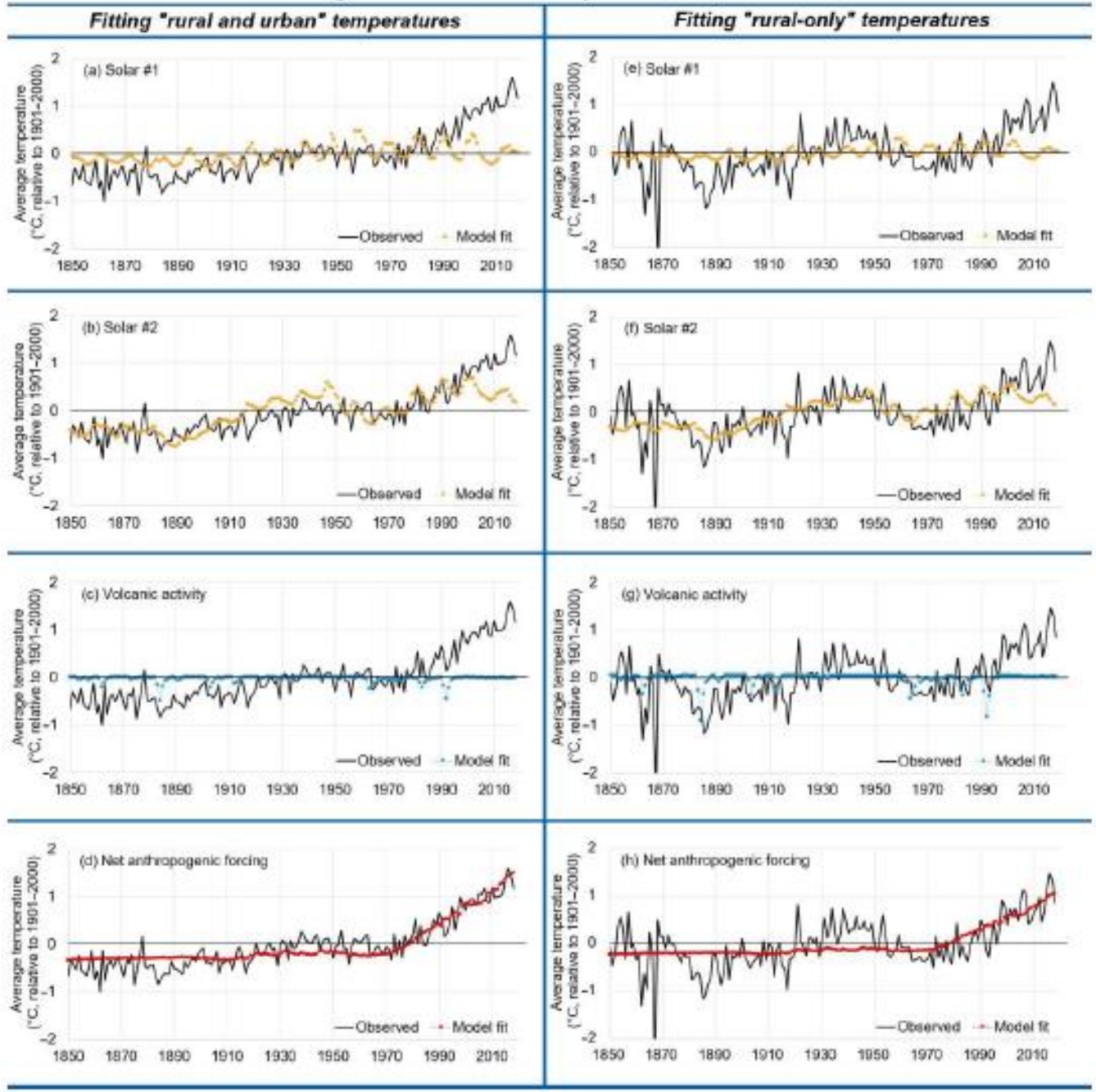

Figure 7. The results of fitting (**a**–**d**) the "rural *and* urban" or (**e**–**h**) the "rural-only" temperature records (indicated by thick black lines) using only one component (using ordinary least squares linear regression) over the 1850–2018 period. The best fits for each individual component are indicated in each panel with colored circles joined by a dotted line. (**a**,**e**) show the best fits for Solar #1; (**b**,**f**) show the best fits for Solar #2; (**c**,**g**) show the best fits for volcanic; (**d**,**h**) show the best fits for the net anthropogenic forcing.

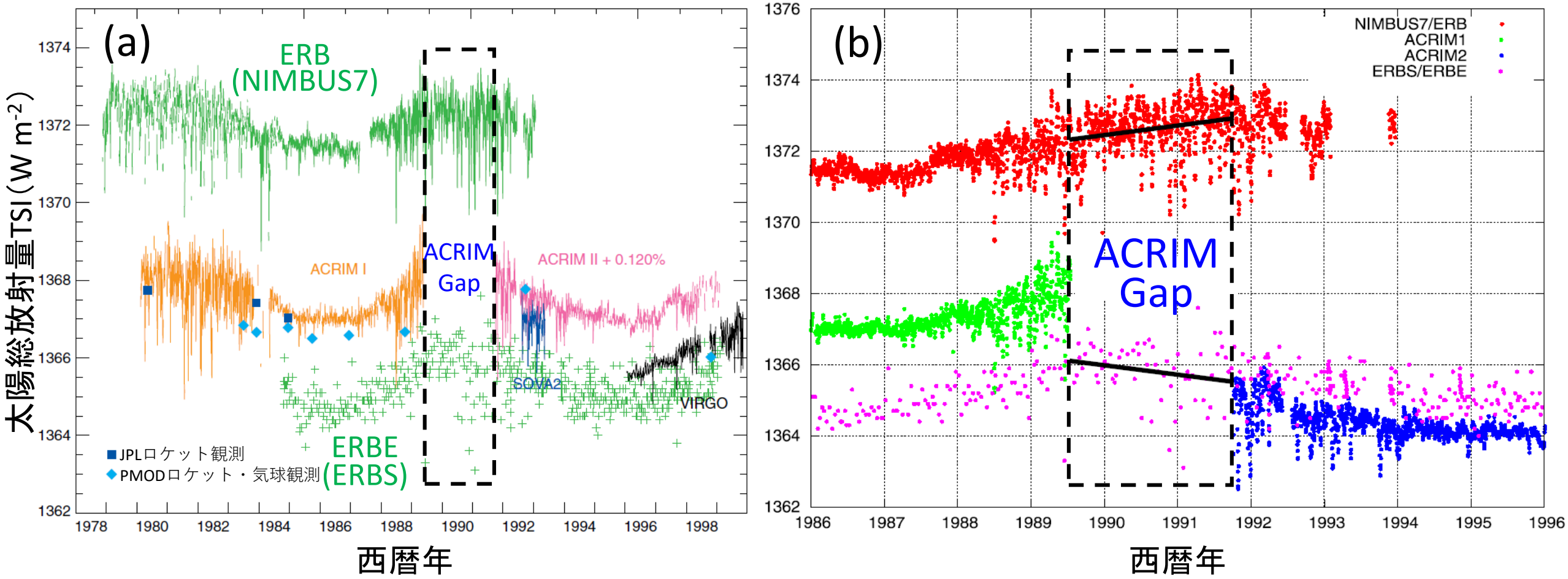

図2　(a)1979～1999年における様々な人工衛星・ロケット・気球観測による太陽総放射量TSI（Ramaswamy et al., 2001）と1986～1996年におけるACRIM1・ACRIM2・ERBおよびERBEによる観測結果の経年変化（Scafetta and Willson, 2014）。(b)の黒線はACRIM-Gap期間におけるERBおよびERBSの線形回帰直線。

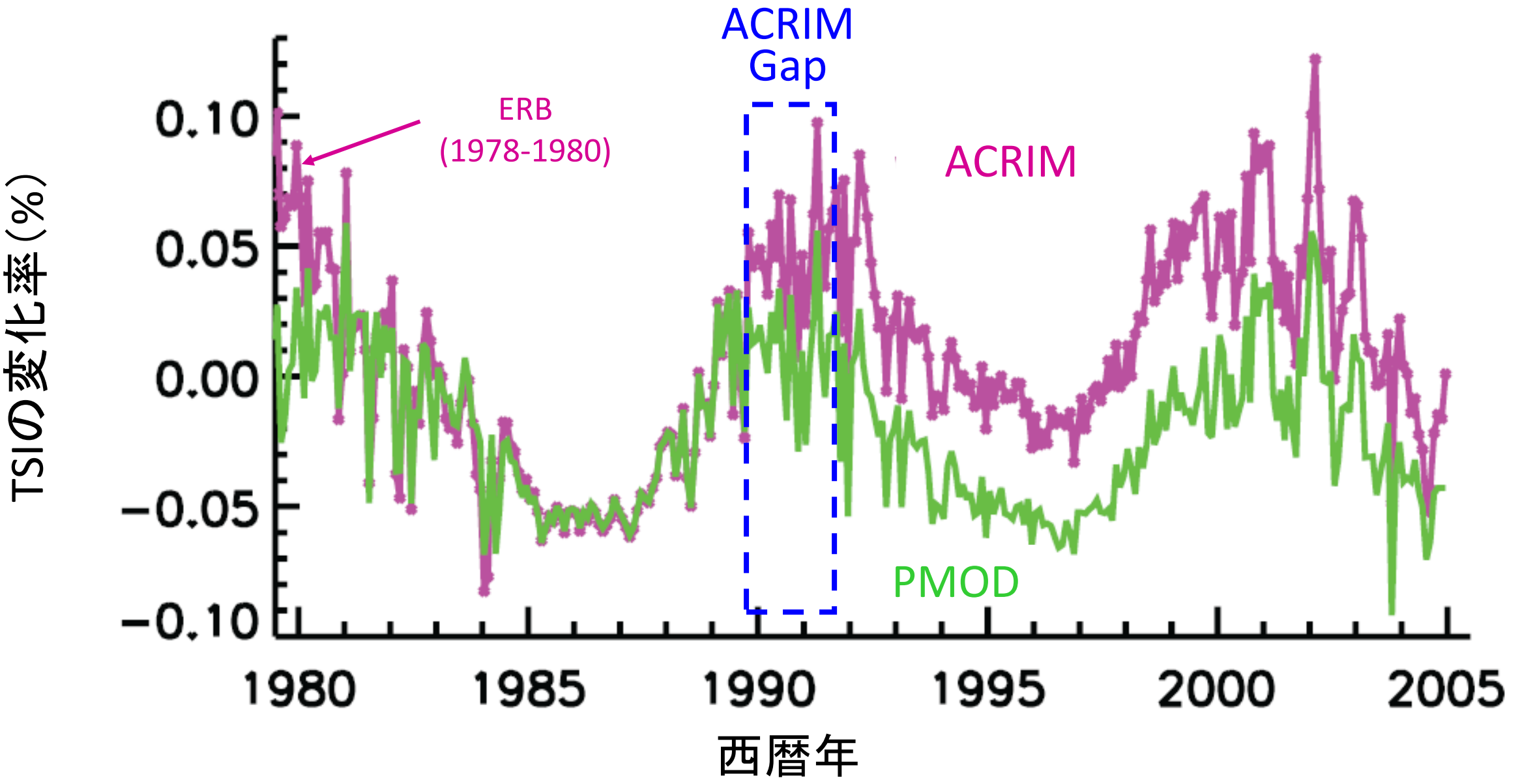

図3　1980年～2005年の平均値を基準としたACRIMデータセット（Willson and Mordvinov, 2003）およびPMODデータセット（Fröhlich and Lean, 2004）による月平均太陽総放射量TSIの変化率（Forster et al., 2007）。1978年～1980年のACRIMデータセットはERBによる観測結果。

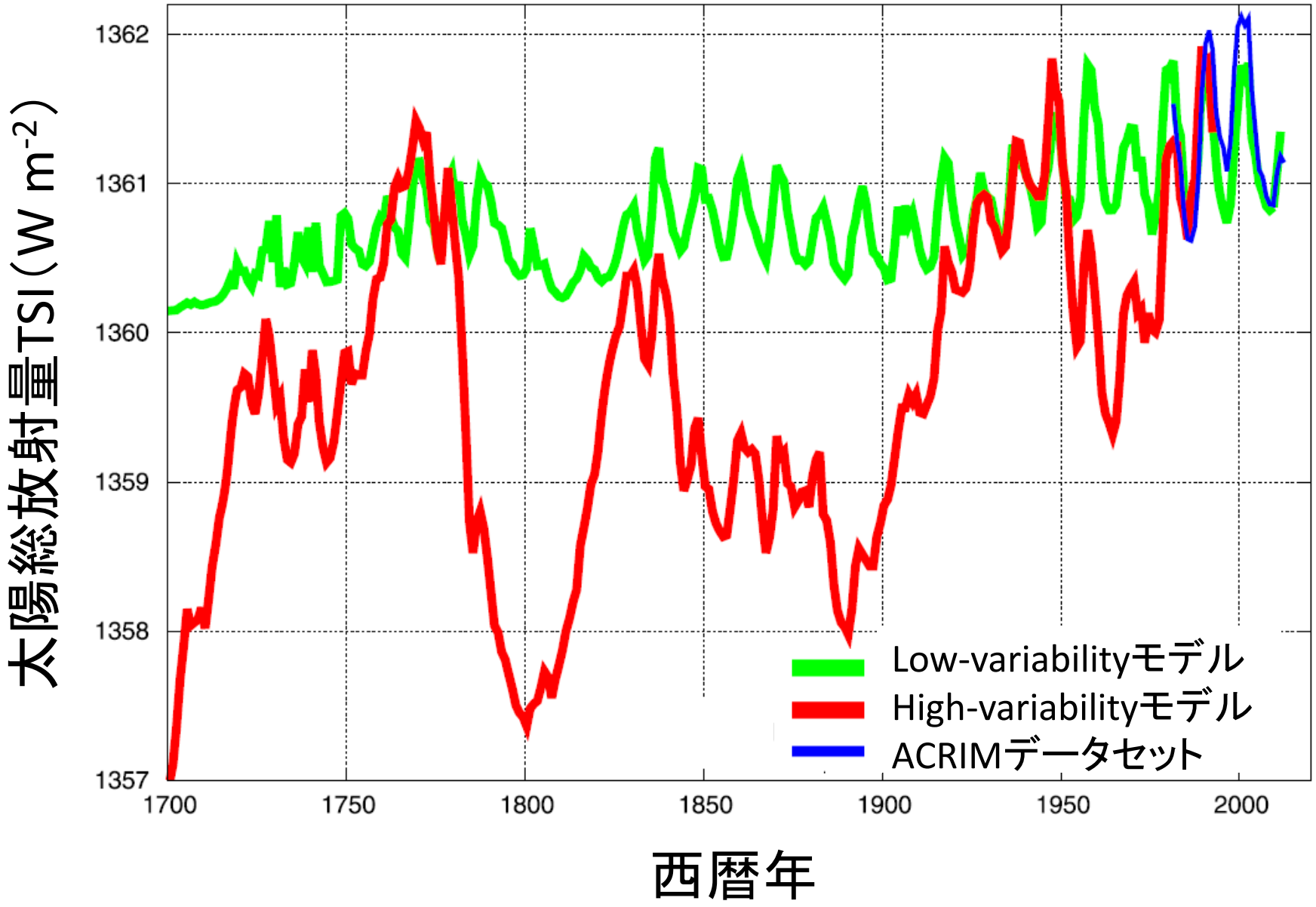

図4　1700年～2004年のLow-variabilityモデル（Kopp and Lean, 2011）とHigh-variabilityモデル（Hoyt and Schatten, 1993の補正値）による太陽総放射量（TSI）の推定結果とACRIMデータセットによる観測値の経年変化（Scafetta and Willson, 2014）。

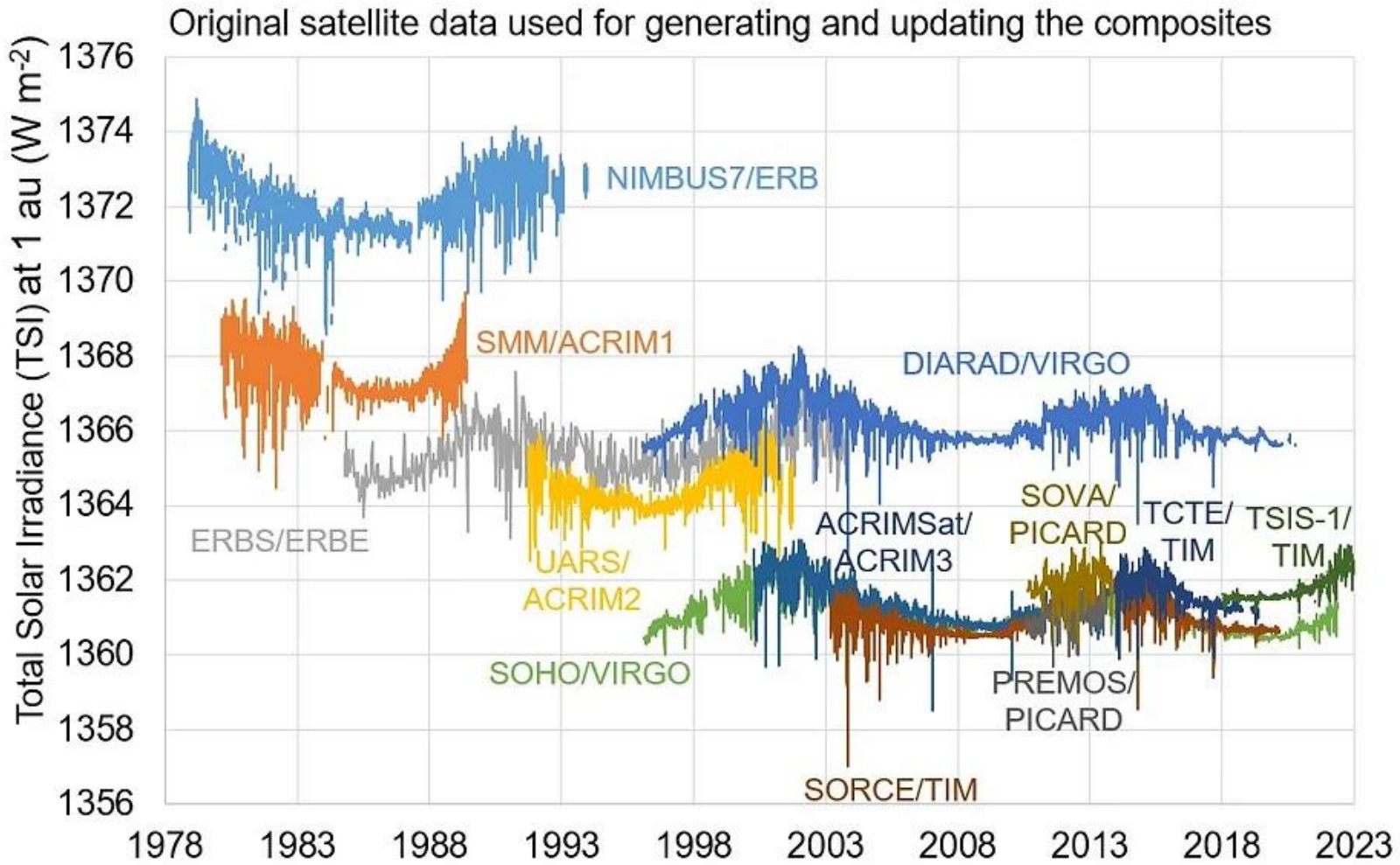

We can see from the above that, even though the data from each satellite mission are different, all of the instruments record the increases and decreases in solar activity over the roughly 11 year "solar cycle" which is observed in many solar activity indicators.

- Detailed assessment of the influence of the many operational interruptions in the ACRIM-II record (*Fröhlich*, 2004).

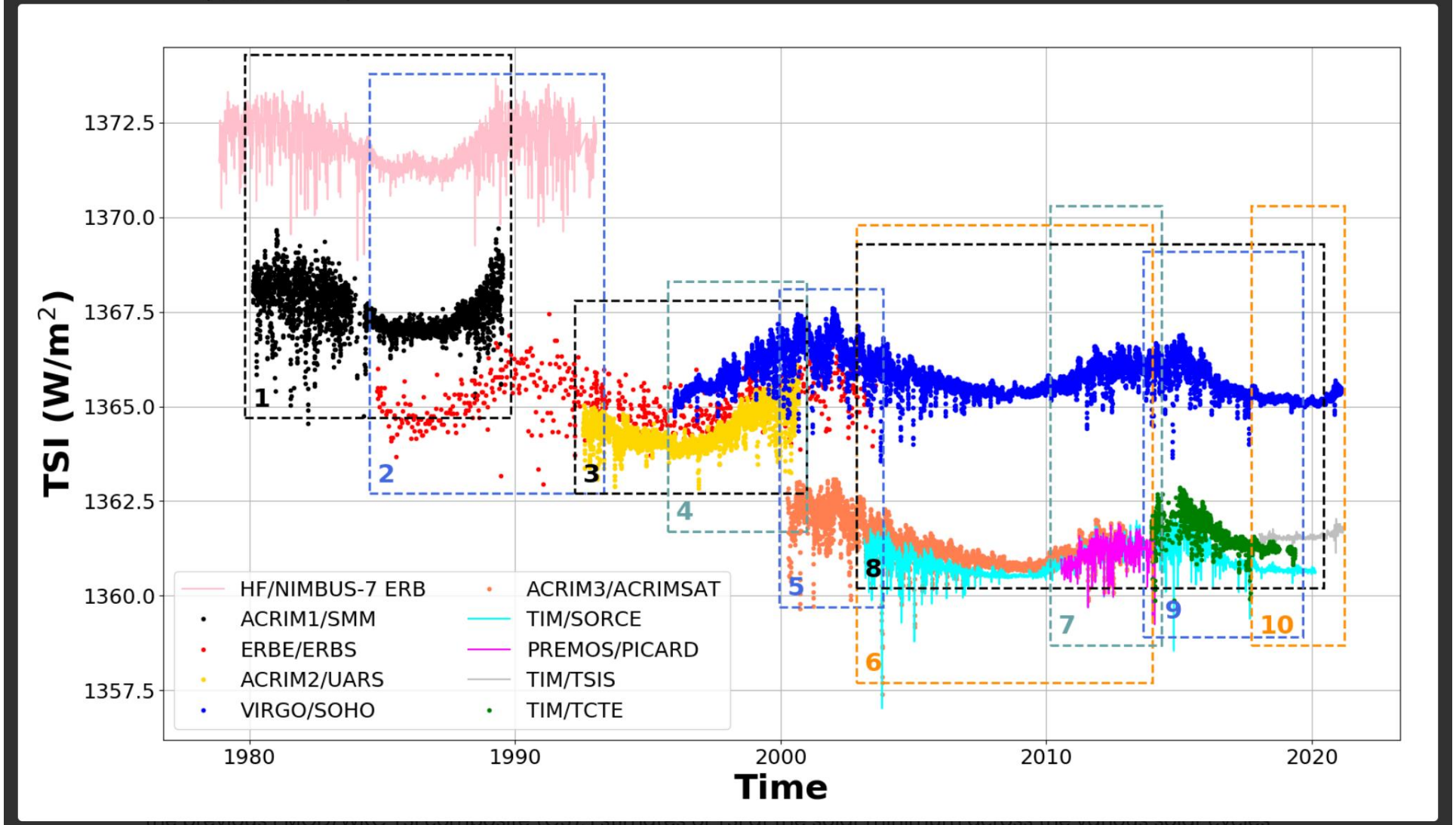

Solar Physics: TSI composite Fig1

from 1980 to the present are shown in Table 2.

Table 2. Estimate of TSI at the solar minimum during the last 41 years from the TSI time-series (mean μ and standard deviation σ) released by *Dudok de Wit et al.* (2017) (C1), by *Dewitte and Nevens* (2016) (C2) and by *Frohlich* (2006) (C3). The new TSI composite is referred to as CPMDFI, and after using the wavelet filter, to CPMDF2. The difference in irradiance between solar minima (SM) from consecutive solar cycles (e.g., ΔI22/23-21/22) is also displayed with the uncertainties (bold text).

以下は予

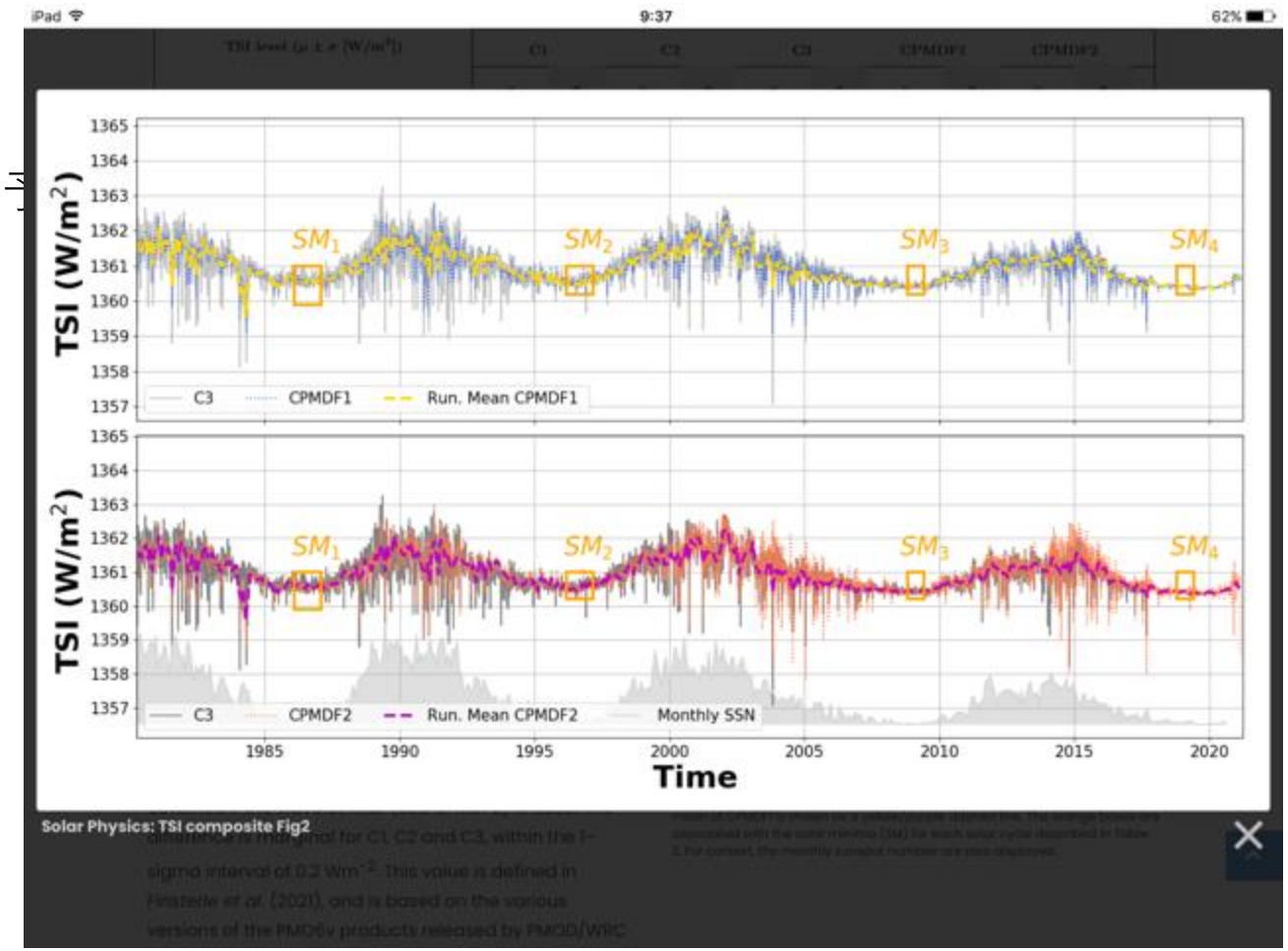
iPad
9:37
62%
TSI (W/m^2)
1365
1364
1363
1362
1361
1360
1359
1358
1357
SM_1
SM_2
SM_3
SM_4
C3
CPMDF1
Run. Mean CPMDF1
TSI (W/m^2)
C3
CPMDF2
Run. Mean CPMDF2
Monthly SSN
1985
1990
1995
2000
2005
2010
2015
2020
Time
Solar Physics: TSI composite Fig2

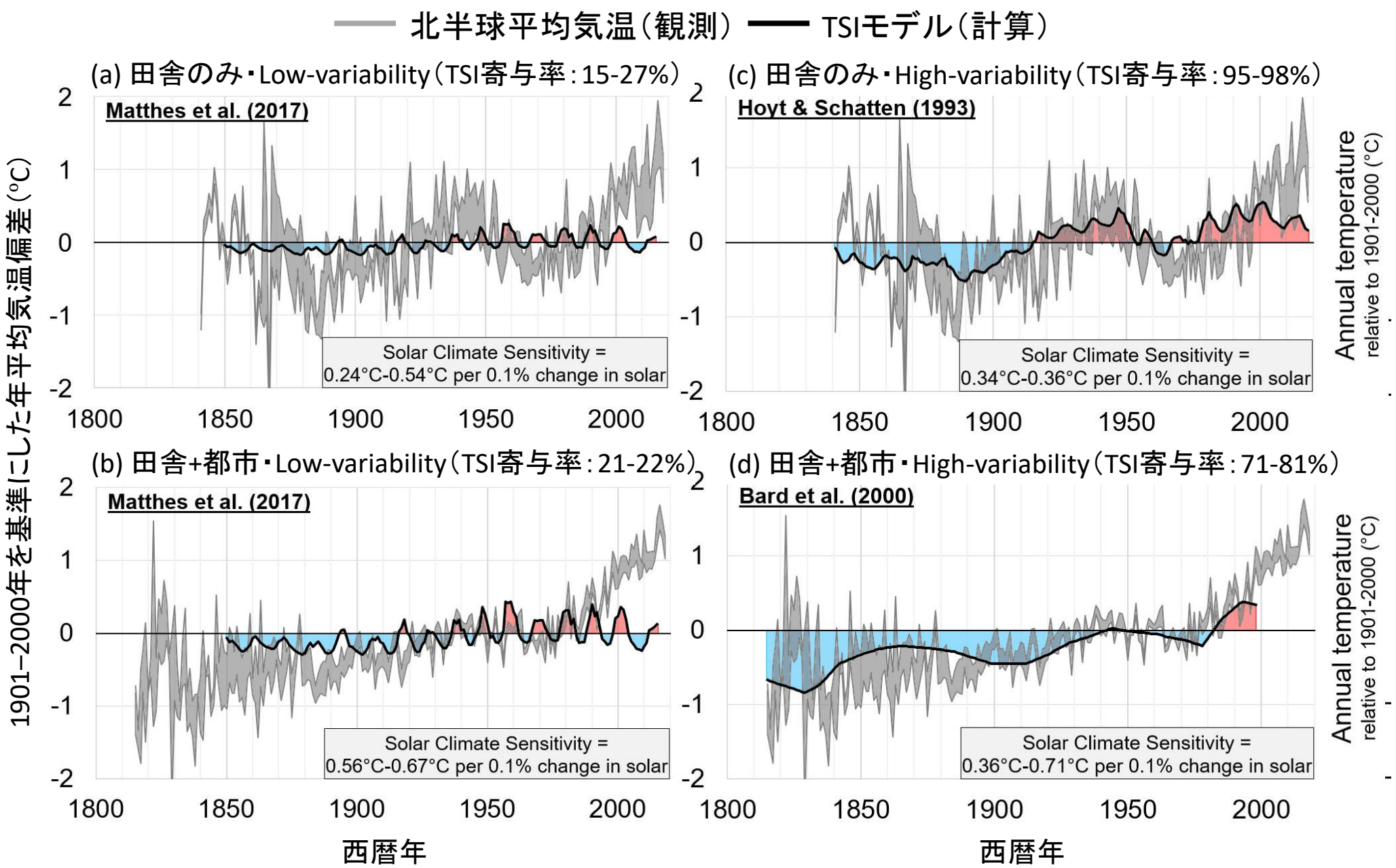

図5(a, c)1800年～2014年における北半球の田舎のみの観測地点および(b, d)全観測地点（田舎・都市両方）の年平均気温の観測結果とLow-variabilityモデル・High-variabilityモデルによる太陽総放射量（TSI）の計算結果の時系列変化（Connolly et al., 2021）。TSIの計算結果は最小二乗法により気温観測値にフィッティングすることで縦軸のスケールを合わせている。

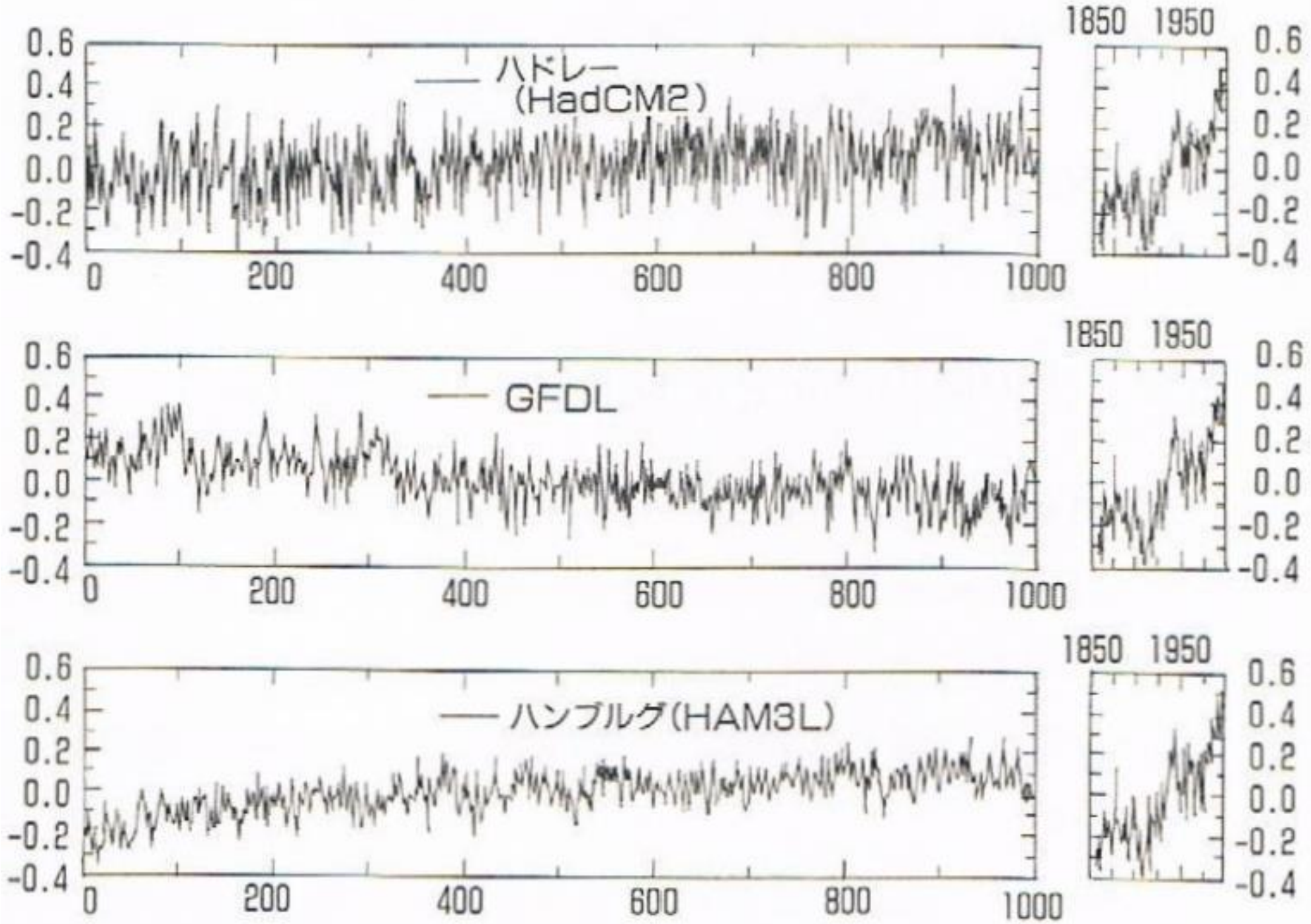
ハドレー
(HadCM2)
GFDL
ハンブルグ(HAM3L)
0.6
0.4
0.2
0.0
-0.2
-0.4
0
200
400
600
800
1000
1850
1950

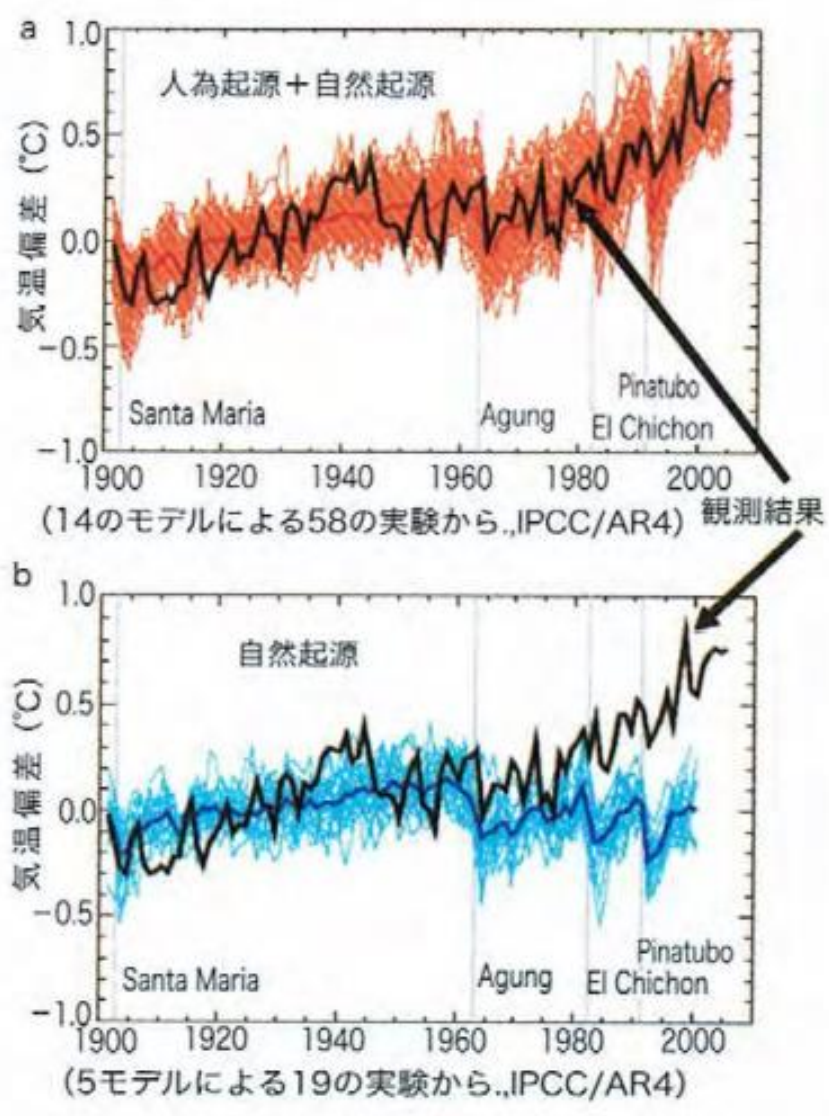

図 1　IPCC 報告による人為的地球温暖化の検証実験（近藤 2009）[3]

以下は予備

Evaluation metrics

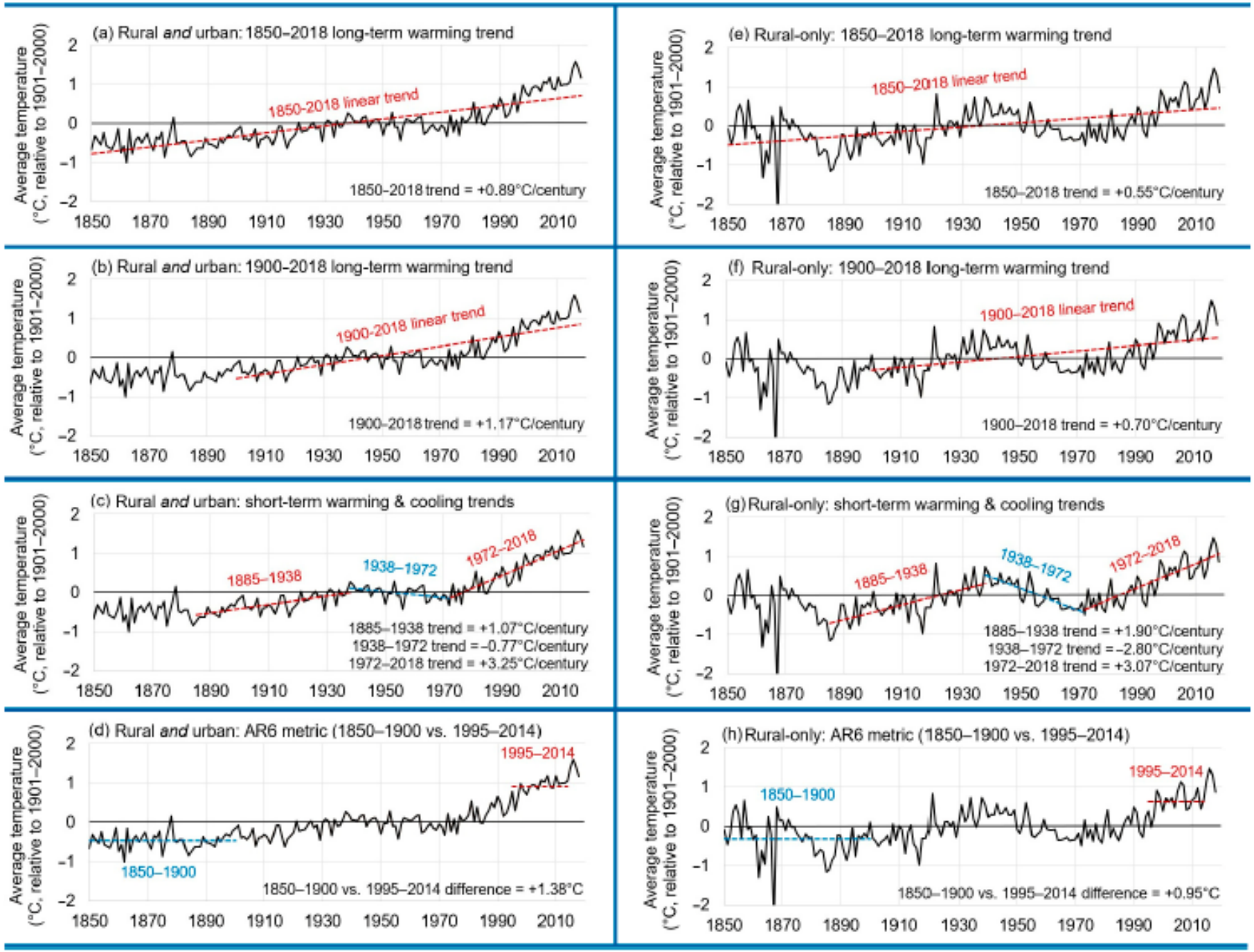

Figure 5. Illustration of the four evaluation metrics when applied to (**a**–**d**) the estimates of Northern Hemisphere land surface air temperatures derived from both rural and urban stations and (**e**–**h**) the estimates derived from only rural stations. (**a**,**e**) show the long-term linear trend over the entire period of record, i.e., 1850–2018. (**b**,**f**) show the linear trends over our secondary period analysis, i.e., 1900–2018. (**c**,**g**) show three shorter-term warming and cooling periods associated with both time series since the late-19th century, i.e., warming between 1885–1938 and 1972–2018 and a cooling period between 1938–1972. (**d**,**h**) show the "AR6" metric, i.e., a comparison between the average temperatures for 1850–1900 and 1995–2014.

Fitting functions for each component

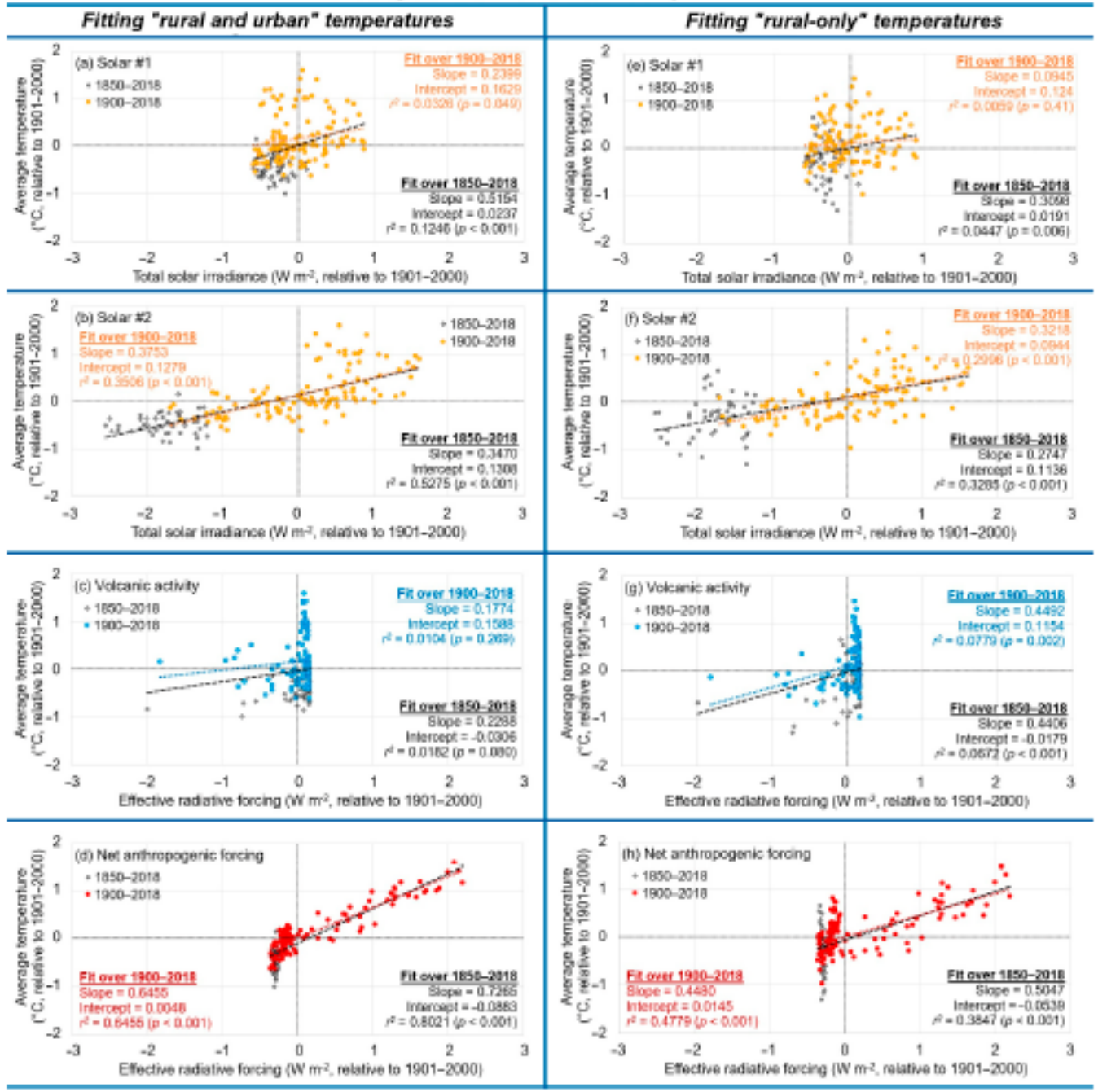

Figure 6. The ordinary least squares linear regression fitting functions between (**a**–**d**) the "rural *and* urban" temperature record and (**e**–**h**) the "rural-only" temperature record. For the 1850–2018 period, the data are shown with gray diamonds; the linear fits are shown with black dashed lines. For the 1900–2018 period, the data are shown with colored circles; the linear fits are shown with colored dotted lines. The slopes and intercepts of each linear relationship along with the r^2 and p statistics of the fits are shown in the relevant panel with the 1850–2018 statistics indicated by black text and those for the 1900–2018 indicated by colored text.

Table 1. Results of individual component analysis fitting of the "rural and urban" temperature record over the 1850–2018 period in terms of the various evaluation metrics.

Evaluation Metric	Rural *and* Urban	Solar #1	Solar #2	Volcanic	Anthropogenic
Trend-based	Trend (°C/century)	%	%	%	%
1850–2018	0.89	21%	70%	0%	82%
1900–2018	1.17	15%	39%	−2%	107%
1885–1938	1.07	28%	201%	8%	21%
1938–1972	−0.77	−32%	222%	35%	18%
1972–2018	3.25	−7%	18%	4%	109%
Period-based	Difference (°C)				
AR6	1.37	12%	66%	2%	88%

Table 2. Results of individual component analysis fitting of the "rural-only" temperature record over the 1850–2018 period in terms of the various evaluation metrics.

Evaluation Metric	Rural-Only	Solar #1	Solar #2	Volcanic	Anthropogenic
Trend-based	Trend (°C/century)	%	%	%	%
1850–2018	0.55	20%	89%	−2%	93%
1900–2018	0.70	16%	53%	−6%	124%
1885–1938	1.90	9%	89%	9%	8%
1938–1972	−2.80	−5%	49%	19%	3%
1972–2018	3.07	−4%	15%	8%	80%
Period-based	Difference (°C)				
AR6	0.95	9%	75%	4%	87%

Table 3. Results of multiple linear regression fitting of the "rural and urban" temperature record over the 1850–2018 period in terms of the various evaluation metrics.

Evaluation Metric	Rural *and* Urban	Scenario 1	Scenario 2	Scenario 3	Scenario 4
Trend-based	Trend (°C/century)	%	%	%	%
1850–2018	0.89	87%	92%	21%	70%
1900–2018	1.17	108%	100%	15%	38%
1885–1938	1.07	38%	100%	28%	206%
1938–1972	−0.77	38%	129%	−32%	247%
1972–2018	3.25	106%	98%	−7%	21%
Period-based	Difference (°C)				
AR6	1.37	91%	97%	12%	66%

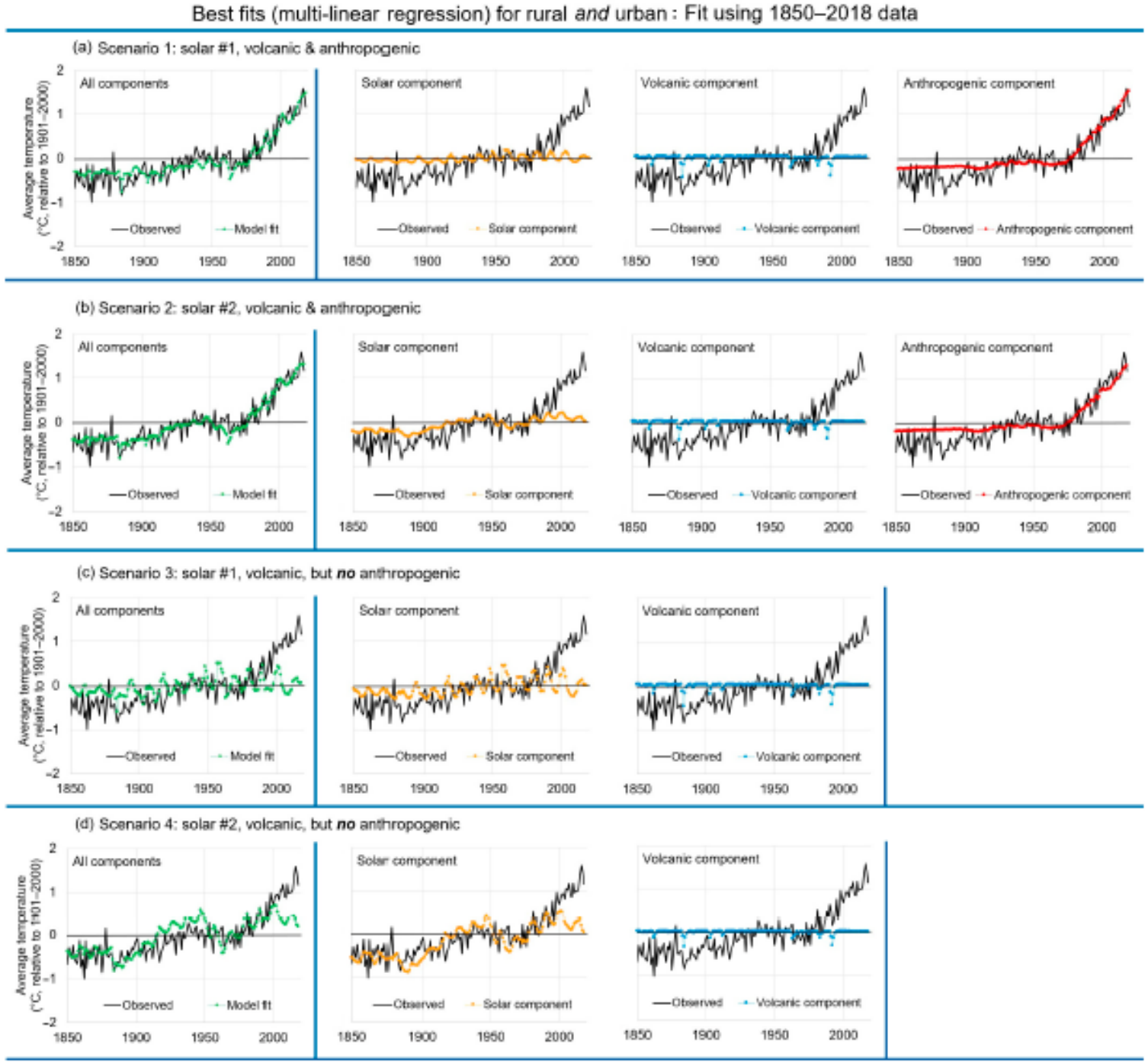
Best fits (multi-linear regression) for rural *and* urban : Fit using 1850–2018 data
(a) Scenario 1: solar #1, volcanic & anthropogenic
(b) Scenario 2: solar #2, volcanic & anthropogenic
(c) Scenario 3: solar #1, volcanic, but **no** anthropogenic
(d) Scenario 4: solar #2, volcanic, but **no** anthropogenic
All components
Solar component
Volcanic component
Anthropogenic component
Average temperature (°C, relative to 1901–2000)
Observed
Model fit
Solar component
Volcanic component
Anthropogenic component
1850
1900
1950
2000

Figure 8. The results of fitting the temperature records over the entire 1850–2018 period using multiple components (using ordinary least squares multiple linear regression) for the "rural *and* urban" temperature record. (**a**–**d**) show the best fits for Scenarios 1–4, respectively. The temperature record is shown in each panel by a thick black line. The panels on the left-hand-side show the model fits with green colored circles joined by a dotted line. The other panels show the contribution to the model fit from each of the two or three components.

Best fits (multi-linear regression) for rural *and* urban : Fit using 1850–2018 data

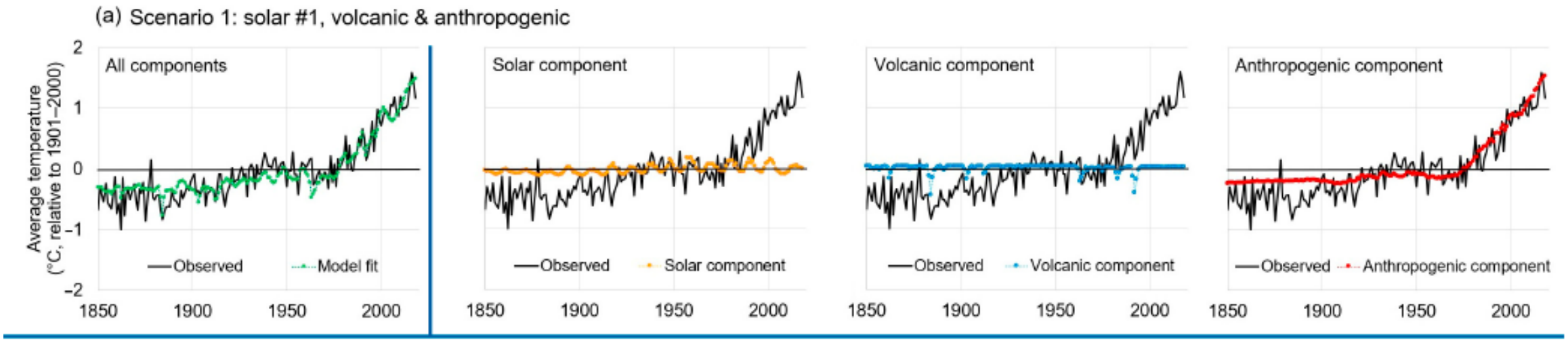

(b) Scenario 2: solar #2, volcanic & anthropogenic

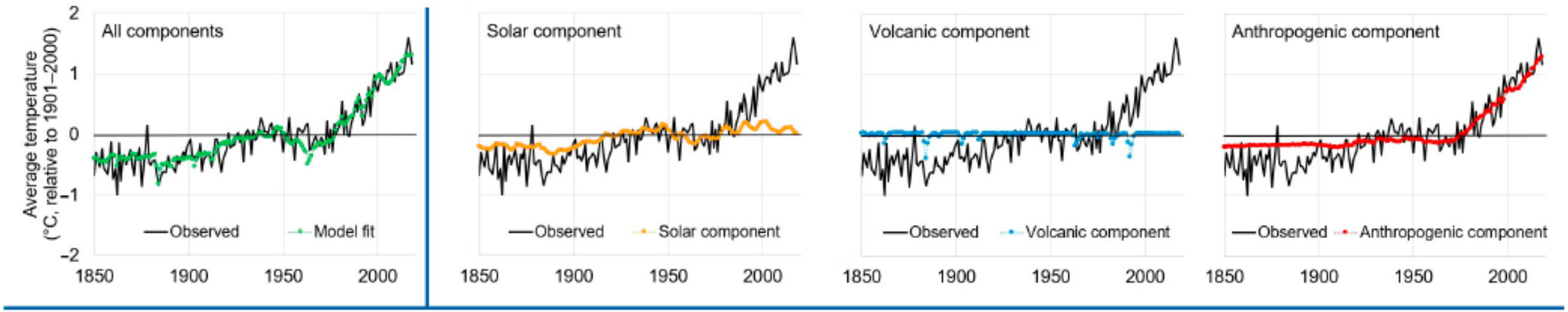

(c) Scenario 3: solar #1, volcanic, but ***no*** anthropogenic

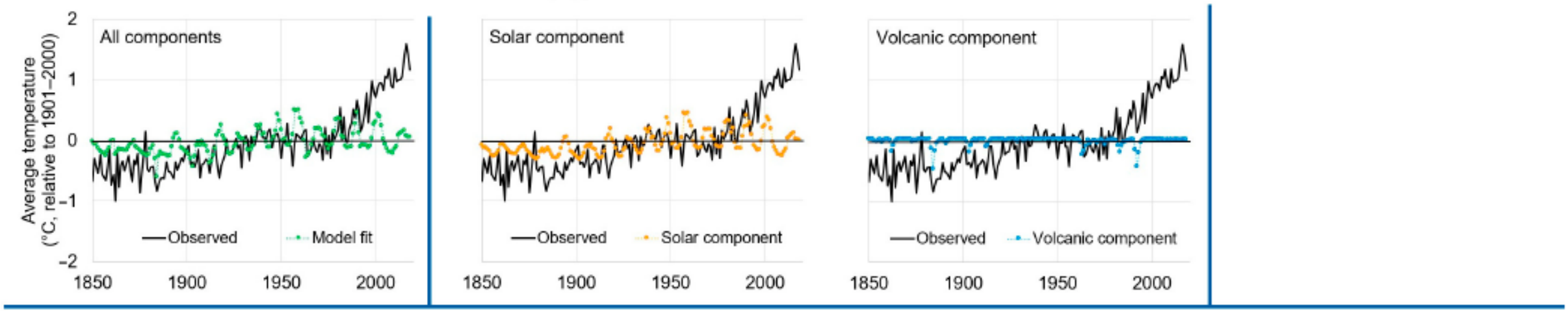

(d) Scenario 4: solar #2, volcanic, but ***no*** anthropogenic

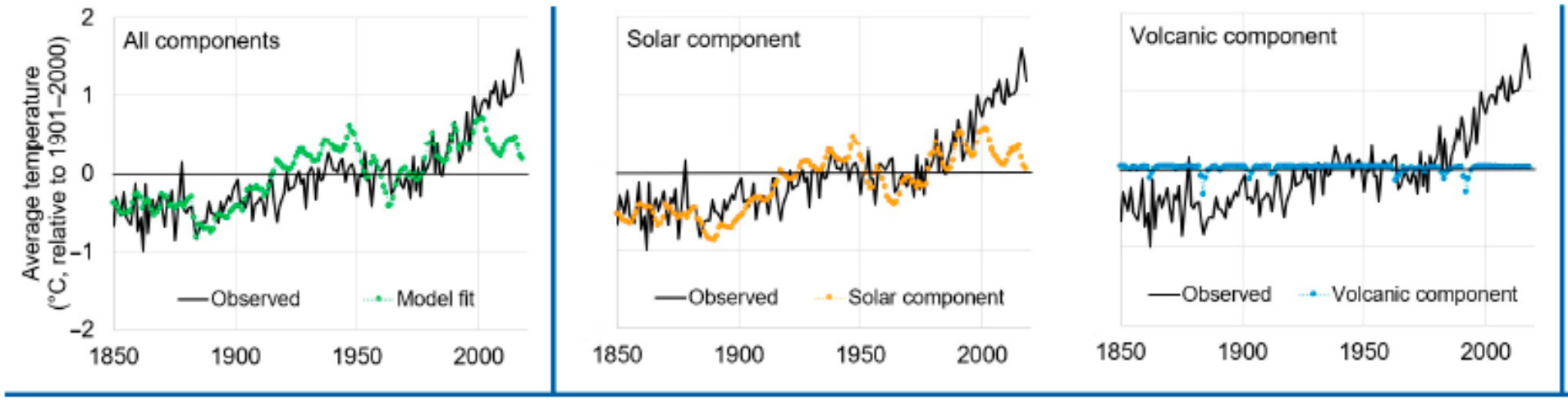

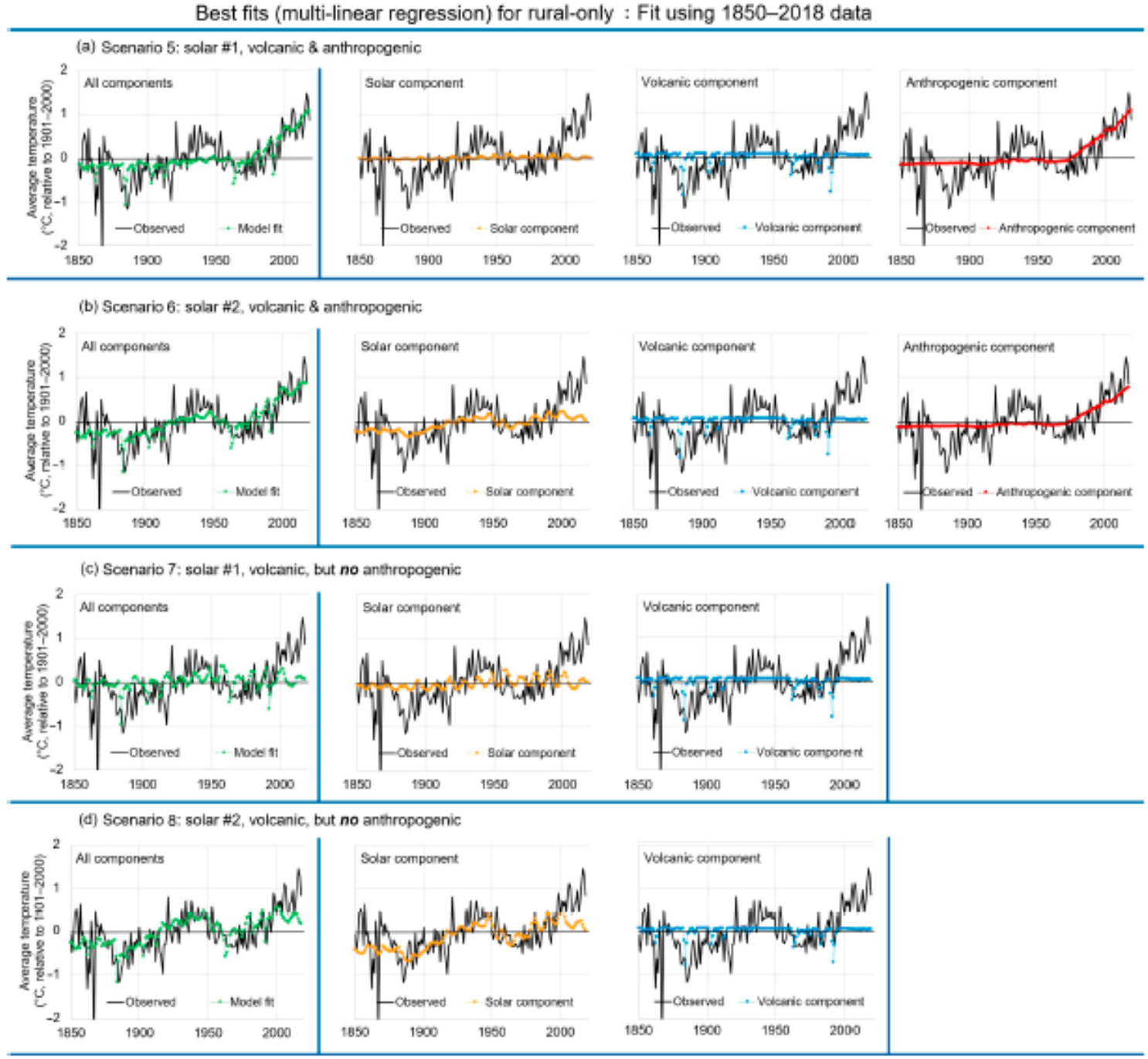
Best fits (multi-linear regression) for rural-only : Fit using 1850–2018 data
(a) Scenario 5: solar #1, volcanic & anthropogenic
(b) Scenario 6: solar #2, volcanic & anthropogenic
(c) Scenario 7: solar #1, volcanic, but no anthropogenic
(d) Scenario 8: solar #2, volcanic, but no anthropogenic
All components
Solar component
Volcanic component
Anthropogenic component
Average temperature (°C, relative to 1901–2000)
Observed
Model fit
Volcanic compone nt
1850
1900
1950
2000

Figure 9. As for Figure 8, except for the "rural-only" temperature records. The results of fitting the temperature records over the entire 1850–2018 period using multiple components (using ordinary least squares multiple linear regression) for the "rural-only" temperature record. (**a**–**d**) show the best fits for Scenarios 1–4 respectively. The temperature record is shown in each panel by a thick black line. The panels on the left-hand-side show the model fits with green colored circles joined by a dotted line. The other panels show the contribution to the model fit from each of the two or three components.

Best fits (multi-linear regression) for rural-only : Fit using 1850–2018 data

(a) Scenario 5: solar #1, volcanic & anthropogenic

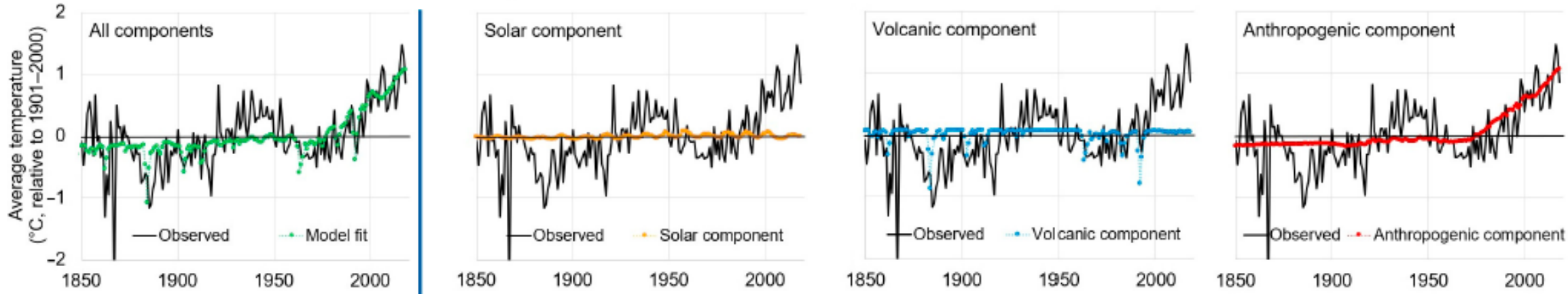

(b) Scenario 6: solar #2, volcanic & anthropogenic

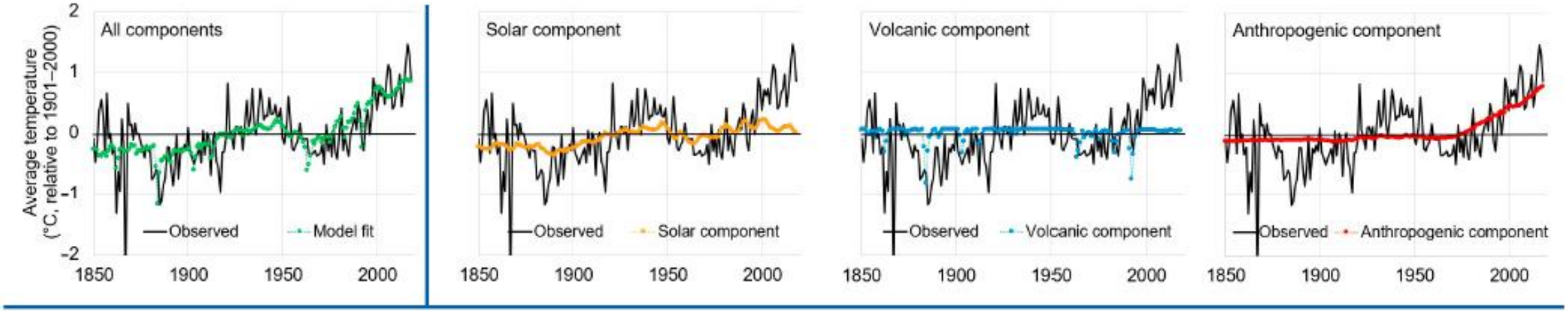

(c) Scenario 7: solar #1, volcanic, but ***no*** anthropogenic

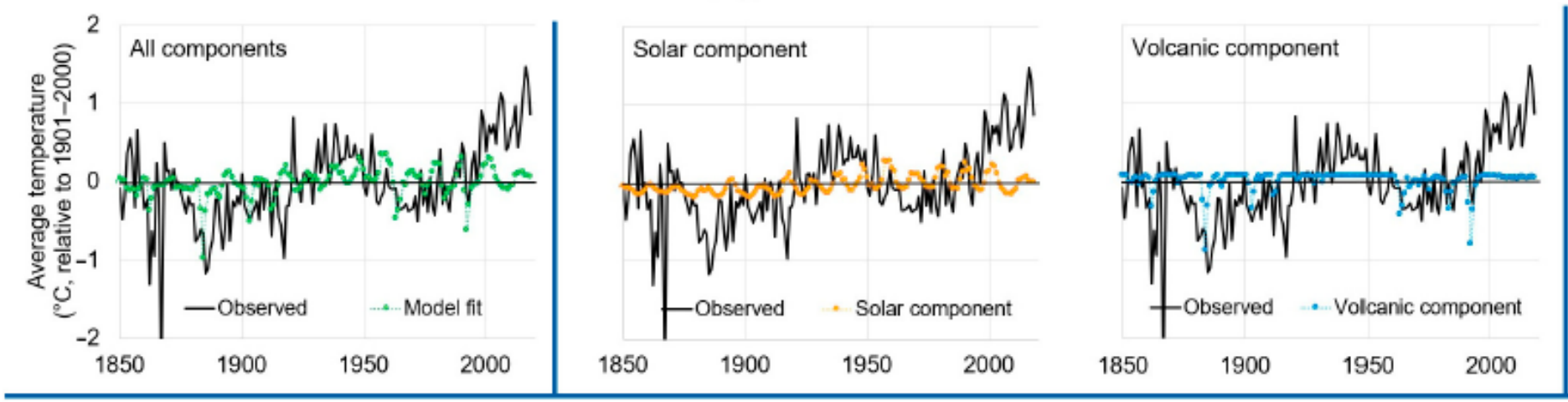

(d) Scenario 8: solar #2, volcanic, but ***no*** anthropogenic

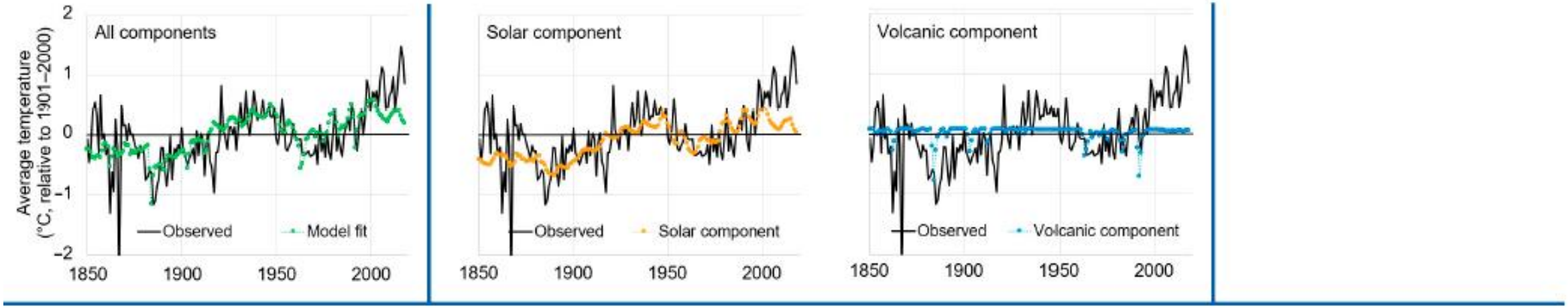

Table 4. Results of multiple linear regression fitting of the "rural-only" temperature record over the 1850–2018 period in terms of the various evaluation metrics.

Evaluation Metric	Rural-Only	Scenario 5	Scenario 6	Scenario 7	Scenario 8
Trend-based	Trend (°C/century)	%	%	%	%
1850–2018	0.55	95%	109%	18%	87%
1900–2018	0.7	120%	110%	11%	47%
1885–1938	1.9	19%	59%	18%	96%
1938–1972	−2.8	20%	44%	13%	64%
1972–2018	3.07	85%	72%	4%	22%
Period-based	Difference (°C)				
AR6	0.95	94%	105%	16%	78%